USAFSAM-TR-88-10

EFFICACY OF CONVENTIONAL AND HIGH-FREQUENCY VENTILATION AT ALTITUDE

Robert A. Klocke, M.D.
Alan T. Aquilina, M.D.
Brydon J.B. Grant, M.D.
Alan R. Saltzman, M.D.
Patricia A. Land, Captain, USAF, NC (USAFSAM/VNC)
Neel B. Ackerman, Jr., Major, USAF, MC (USAFSAM/VNC)

Department of Medicine
Pulmonary Division
State University of New York at Buffalo
Buffalo, NY 14214

December 1988

Final Report for Period July 1985 - December 1986

Prepared for
USAF SCHOOL OF AEROSPACE MEDICINE
Human Systems Division (AFSC)
Brooks Air Force Base, TX 78235-5301

NOTICES

This final report was submitted by the Department of Medicine, Pulmonary Division, State University of New York at Buffalo, Buffalo, New York, under contract F33615-83-D-0601, job order 7930-16-04, with the USAF School of Aerospace Medicine, Human Systems Division, AFSC, Brooks Air Force Base, Texas. Second Lieutenant Sue K. Nagel (USAFSAM/VNC) was the Laboratory Project Scientist-in-Charge.

When Government drawings, specifications, or other data are used for any purpose other than in connection with a definitely Government-related procurement, the United States Government incurs no responsibility or any obligation whatsoever. The fact that the Government may have formulated or in any way supplied the said drawings, specifications, or other data, is not to be regarded by implication, or otherwise in any manner construed, as licensing the holder or any other person or corporation; or as conveying any rights or permission to manufacture, use, or sell any patented invention that may in any way be related thereto.

The animals involved in this study were procured, maintained, and used in accordance with the Animal Welfare Act and the "Guide for the Care and Use of Laboratory Animals" prepared by the Institute of Laboratory Animal Resources-National Research Council.

The Office of Public Affairs has reviewed this report, and it is releasable to the National Technical Information Service, where it will be available to the general public, including foreign nationals.

This report has been reviewed and is approved for publication.

SUE K. NAGEL, 2d Lieutenant, USAF, BSC
Project Scientist

F. WESLEY KAUMGARDNER, Ph.D.
Supervisor

JEFFREY G. DAVIS, Colonel, USAF, MC
Commander

UNCLASSIFIED
SECURITY CLASSIFICATION OF THIS PAGE

REPORT DOCUMENTATION PAGE

Form Approved OMB No. 0704-0188

1a REPORT SECURITY CLASSIFICATION: Unclassified	1b RESTRICTIVE MARKINGS:
2a SECURITY CLASSIFICATION AUTHORITY:	3 DISTRIBUTION/AVAILABILITY OF REPORT: Approved for public release; distribution is unlimited.
2b DECLASSIFICATION/DOWNGRADING SCHEDULE:	
4 PERFORMING ORGANIZATION REPORT NUMBER(S):	5 MONITORING ORGANIZATION REPORT NUMBER(S): USAFSAM-TR-88-10
6a NAME OF PERFORMING ORGANIZATION: Dept. of Medicine, Pulmonary Division; 6b OFFICE SYMBOL (If applicable):	7a NAME OF MONITORING ORGANIZATION: USAF School of Aerospace Medicine (VNC)
6c ADDRESS (City, State, and ZIP Code): State University of New York at Buffalo, Buffalo, NY 14214	7b ADDRESS (City, State, and ZIP Code): Human Systems Division (AFSC), Brooks AFB, TX 78235-5301
8a NAME OF FUNDING/SPONSORING ORGANIZATION: ; 8b OFFICE SYMBOL (If applicable):	9 PROCUREMENT INSTRUMENT IDENTIFICATION NUMBER: F33615-83-D-0601
8c ADDRESS (City, State, and ZIP Code):	10 SOURCE OF FUNDING NUMBERS: PROGRAM ELEMENT NO: 62202F; PROJECT NO: 7930; TASK NO: 16; WORK UNIT ACCESSION NO: 04

11 TITLE (Include Security Classification)

Efficacy of Conventional and High-Frequency Ventilation at Altitude

12 PERSONAL AUTHOR(S) Klocke, Robert A.; Aquilina, Alan T.; Grant, Brydon J. B.; Saltzman, Alan R.; Land, Patricia A. (USAFSAM); Ackerman, Neel B., Jr. (USAFSAM)

13a TYPE OF REPORT	13b TIME COVERED	14 DATE OF REPORT (Year, Month, Day)	15 PAGE COUNT
Final	FROM 85/07 TO 86/12	1988, December	53

16 SUPPLEMENTARY NOTATION

17 COSATI CODES		
FIELD	GROUP	SUB-GROUP
06	11	
06	12	

18 SUBJECT TERMS (Continue on reverse if necessary and identify by block number)
Aeromedical evacuation; Ventilatory requirements; Air evacuation; Mechanical ventilation; and High-Frequency ventilation; (KT)

19 ABSTRACT (Continue on reverse if necessary and identify by block number)

High-frequency ventilation (HFV) is a promising mode of ventilatory support and could be useful in aeromedical evacuation. There have been no studies to date to examine the feasibility of maintaining gas exchange with HFV at reduced barometric pressure. This report investigates (1) the role of molecular diffusion in gas transport during HFV, and (2) the ability to maintain gas exchange with HFV at simulated altitude in healthy and in diseased lungs. The role of molecular diffusion was tested by determining the rate of pulmonary uptake of six tracer gases with low aqueous solubility but different molecular weights during conventional and high-frequency ventilation. The inspired gas and the subsequent rate of appearance of these gases in arterial blood were monitored. With conventional mechanical ventilation (CMV), there was separation of the gases with appearance in arterial blood occurring in order of increasing molecular weight. With HFV, there was a slight molecular weight effect, but substantially less than that seen with CMV. These findings indicate that the role of molecular diffusion during HFV is minimal, but a significantly greater effect of diffusion is present during CMV.

20 DISTRIBUTION/AVAILABILITY OF ABSTRACT	21 ABSTRACT SECURITY CLASSIFICATION
☒ UNCLASSIFIED/UNLIMITED ☐ SAME AS RPT ☐ DTIC USERS	Unclassified
22a NAME OF RESPONSIBLE INDIVIDUAL: Sue K. Nagel, 2d Lt, USAF, BSC	22b TELEPHONE (Include Area Code): 512-536-2937 / 22c OFFICE SYMBOL: USAFSAM/VNC

DD Form 1473, JUN 86 — Previous editions are obsolete — SECURITY CLASSIFICATION OF THIS PAGE: UNCLASSIFIED

TABLE OF CONTENTS

	Page
INTRODUCTION	1
EXPERIMENTAL STUDY: PART I	4
Methods	4
Results	19
EXPERIMENTAL STUDY: PART II	28
Methods	28
Results	35
DISCUSSION	42
REFERENCES	56

Figures

Fig. No.		
1.	Experimental preparation	6
2.	Ventilator circuit used for washin during CMV	9
3.	Oscillator circuit used for washin during HFV	11
4.	Valve assembly used in measurements of inert gases	17
5.	Gas concentrations in experiment 1A during washin with CMV	21
6.	Gas concentrations in experiment 1B during washin with HFV	22
7.	Logarithmic plot of fitted exponential relationships for inert gas washin data from experiment 1A conducted with CMV	24
8.	Logarithmic plot of fitted exponential relationships for inert gas washin data from experiment 1B conducted with HFV	25
9.	Relationship between the rate constants fitted to the gas washin data and the inverse square roots of the molecular weights of the gases	26
10.	Circuit used for HFV at ground level and at altitude	29
11.	Mean pulmonary artery pressure at ground level and altitude in normal animals and animals with oleic acid-induced lung injury	41

page

12. Relationship between inspired oxygen tension at ground level and the inspired oxygen fraction required at altitude 54

Tables

Table No.

1. Tracer gases 9

2. Experimental variables: Part I 20

3. Rate constants for gas washin 27

4. Experimental design 34

5. Summary of results 38

EFFICACY OF CONVENTIONAL AND HIGH-FREQUENCY VENTILATION AT ALTITUDE

INTRODUCTION

The logistics of aeromedical evacuation of patients requiring mechanical ventilation is complicated by the design of current ventilators. These instruments, for use at ground level in fixed locations, are bulky, heavy, and may change characteristics of performance at altitude (1). They are entirely unsuitable for field conditions.

Small, lightweight ventilators are needed which will function under less than optimal medical conditions, such as in rugged terrain or during emergency air evacuation. High-frequency ventilators offer an attractive alternative to conventional ventilators and may be better suited to meet these requirements. Unfortunately, little is known concerning the mechanism(s) responsible for adequate gas exchange during high-frequency ventilation (HFV). Further, there are no reports that HFV is effective at reduced barometric pressure. Even though the cabins of military transport aircraft are pressurized, it is not feasible to maintain ambient pressure at usual ground level (760 mmHg) during aeromedical evacuation. At cruising altitudes of 40,000 ft (12,200 m), cabin pressure in most aircraft is equivalent to that present at an elevation of 8,000 ft (2440 m) above sea level (564 mmHg).

Ventilation using the high-frequency mode differs from conventional mechanical ventilation (CMV) in two ways. First, the respiratory rate is considerably greater, ranging from 100 to 2400 breaths/min. In contrast, rates of 6-40 breaths/min are used with CMV. Second, tidal volumes are much smaller than the volumes (10-15 ml/kg) used with conventional ventilation. During HFV, volumes of 1-5 ml/kg are utilized and often are varied inversely as a function of respiratory frequency. In fact, individuals can be ventilated with tidal volumes smaller than the anatomic deadspace of their airways (2).

High-frequency ventilation is usually subdivided into two categories:

(A) High-frequency oscillatory ventilation utilizes a system closed to the environment with small to and fro oscillations applied to the lungs via an endotracheal tube. Airway pressure cycles above and below ambient pressure. Ventilation enters and leaves the lungs only through the endotracheal tube. Respiratory frequencies of 300-2400 breaths/min (5-40 Hz) are utilized to maintain adequate gas exchange. A bias flow of gas is introduced into the system to allow influx of oxygen and removal of carbon dioxide.

(B) High-frequency jet ventilation is accomplished with an open system. Gas under pressure is injected into the trachea via a needle or small tracheostomy tube during the inspiratory phase. Air is also entrained at the tip of the jet injector because the

high velocities at that point produce a Bernoulli effect, drawing in environmental gas via the upper airway. No bias flow is used to introduce gas from the environment. Expiration is passive and negative pressure is not applied by the ventilator during the expiratory phase.

A number of mechanisms have been postulated to be responsible for gas exchange during HFV. These mechanisms include direct alveolar ventilation of lung units located near the airway opening, bulk convective mixing in conductive airways, convective transport resulting from asymmetric inspiratory and expiratory velocity profiles, longitudinal dispersion caused by turbulent eddies, and molecular diffusion in distal compartments near the alveolocapillary membrane (3). These proposed mechanisms depend upon gas movement resulting from laminar flow, turbulent flow, and molecular diffusion. Density is a major determinant of gas movement in the last two conditions. Because gas density varies substantially with ambient pressure (4), changes in environmental pressure may affect the efficacy of HFV. For these reasons, we investigated the importance of diffusion in gas transport with both CMV and HFV, and the feasibility of maintaining normal gas exchange at altitude with HFV in healthy and in diseased lungs.

The role of diffusion in HFV and CMV was studied in healthy animals. Because of the uncertainties of the quantity of total ventilation delivered in high-frequency jet ventilation, we

confined our investigations to HFV achieved with an oscillatory pattern of ventilation.

In the Part I experiments a series of inert tracer gases with differing molecular weights, and therefore differing diffusivities, were introduced suddenly into the inspired stream. Appearance of the gases in arterial blood was monitored by gas chromatography. Because the gases are administered together, they should appear in the blood simultaneously if diffusion plays no role in gas exchange. With increasing diffusion limitation, the gases should separate, and the rate of appearance in the blood would be a function of gas diffusivity.

In the Part II experiments, the feasibility of HFV at altitude was studied by comparing gas exchange in dogs ventilated in the high-frequency mode at both ground level and altitude. Experiments were conducted in healthy animals and in dogs with lung injury induced by intravenous administration of oleic acid. The oleic acid insult produces a lung injury in animals which is similar to the adult respiratory distress syndrome (ARDS) observed in man.

EXPERIMENTAL STUDY: PART I

Methods

Mongrel dogs were initially anesthetized with 4% thiamylal (6 mg/kg), a short acting agent, given by intravenous bolus injection. Deeper and prolonged anesthesia was achieved with an

α-chloralose (120 mg/kg)/sodium tetraborate solution administered as an intravenous bolus immediately after the thiamylal. Maintenance of anesthesia was accomplished with a continuous infusion of α-chloralose (43 mg/kg/h)/sodium tetraborate. A constant-infusion pump was used to maintain an accurate rate of infusion, providing a steady level of anesthesia. α-chloralose is an effective anesthetic agent for non-survival animal experiments, and a single initial dose without continuous supplementation by itself is adequate to provide a surgical level of anesthesia for 6 hours. Pancuronium bromide (0.1 ml/kg) was utilized to provide muscle paralysis. The animal was intubated with a cuffed No. 10 endotracheal tube (34.5 x 1 cm internal diameter) which was connected to either the CMV or HFV respirator.

A femoral intravenous catheter was placed for administration of the anesthetic agent, supplemental fluids, and heparin. An initial dose of 7000 units of heparin was administered, followed by supplemental doses of 3000 units/h to prevent clotting of vascular catheters and avoid the need to heparinize blood samples. A PE 320 (2.69 mm ID) catheter was introduced into the right carotid artery and threaded retrograde into the aortic arch. The arterial catheter was connected to a stopcock which permitted either monitoring blood pressure with a strain gauge (Model P23, Gould, Inc.), or sampling arterial blood via a multi-port manifold (Fig. 1). A Fleisch No. 3

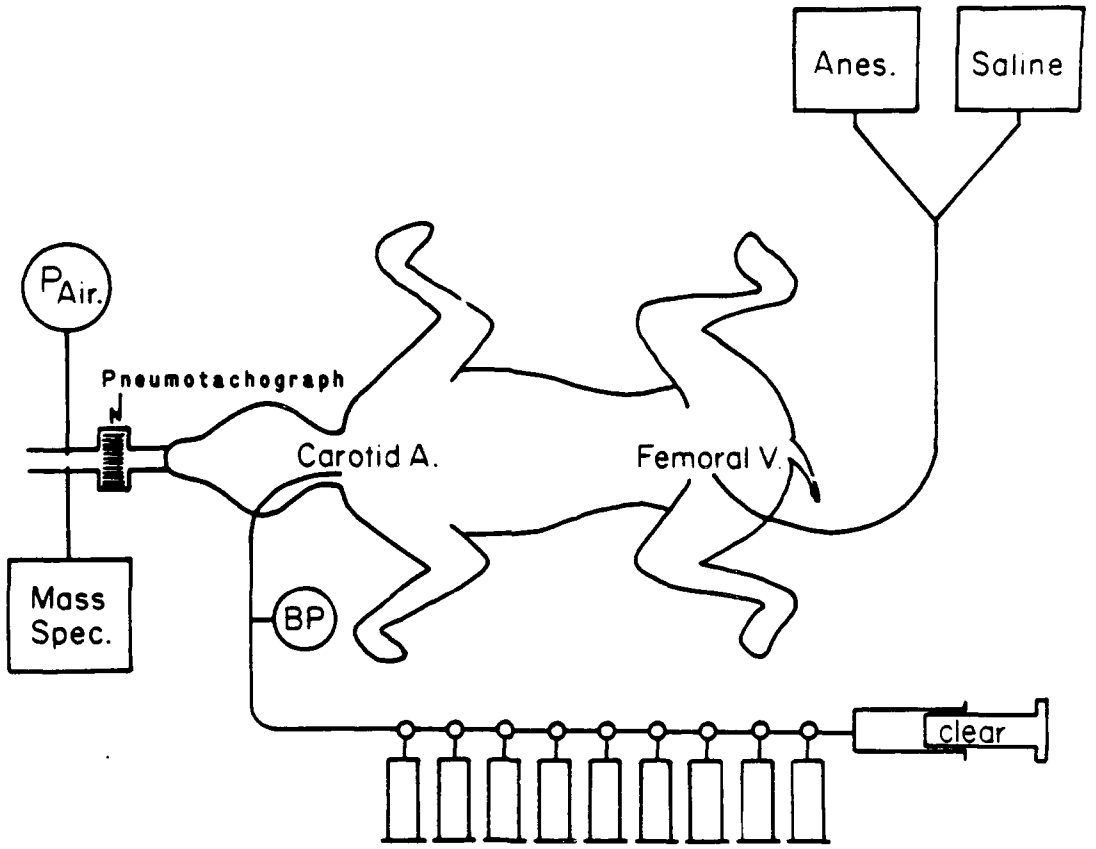

Figure 1. Experimental preparation. P_{Air} = airway pressure transducer; Mass Spec. = mass spectrometer; Anes. = α-chloralose solution; BP = blood pressure transducer; clear = syringe used to withdraw blood to clear the deadspace of the manifold prior to collection of each sample.

pneumotachograph, located between the ventilator and the proximal end of the endotracheal tube, was used to monitor airflow. The pneumotachograph was calibrated by injecting air (3.0 L) from a calibrated syringe at a rate approximately equal to peak airflow and numerically integrating the digitized flow signal as a function of time. The pressure drop across the pneumotachograph was measured with a Validyne MP-45 ($\pm$ 2 cm H_2O) variable reluctance transducer. Airway pressure, monitored with a Validyne MP-45 ($\pm$ 50 cm H_2O) transducer, and instantaneous O_2, CO_2, and N_2 concentrations, obtained with an MGA-1100 Perkin-Elmer mass spectrometer, were measured via ports in the connector between the ventilator and pneumotachograph. The deadspace of the connectors and pneumotachograph between the ventilator and endotracheal tube was 55 ml.

Initially the animals were ventilated with CMV using a dual-piston constant-volume ventilator (Model 618, Harvard Apparatus, Inc.) via a low deadspace valve (11 ml) which permitted rapid changes between the two ventilating pistons (Fig. 2). While one piston was used to ventilate the experimental animal, the tidal volume from the other was exhausted to the atmosphere. Tidal volume was kept constant at 15 ml/kg; respiratory frequency initially was adjusted to maintain a normal arterial Pco_2. Thereafter, no changes were made in the CMV respirator settings.

The inspiratory line of piston A of the CMV ventilator was connected to a non-diffusing gas bag (Calibrated Instruments,

Inc.) filled with 0.1% propane, 30% oxygen, and the balance nitrogen from a pre-mixed gas cylinder (Fig. 2). The inspiratory port of piston B of the dual-piston ventilator was connected to another gas bag containing a similar mixture of propane, oxygen, and nitrogen plus a mixture of tracer gases comprised of hydrogen, helium, methane, ethane, isobutane and sulfur hexafluoride (Table 1). The tracer mixture was made using pure gases from high-pressure cylinders and mixing by volume displacement. Because of the technique used to quantify tracer gases in blood (vide infra), small variations in tracer gas concentrations in the mixture were inconsequential. The addition of the tracer gases caused a slight decrease in O_2, N_2, and C_3H_8 concentrations supplied from the pre-mixed gas cylinder. A small quantity of propane was added to the bag to bring the C_3H_8 concentrations back to the level in the cylinder, but no O_2 or N_2 were added since these changes in concentration were unimportant to the experiment. Propane concentration was measured in both gas bags by gas chromatography and did not differ significantly ($p > 0.8$). Constancy of propane concentration was critical to accurate measurement of tracer gas concentration in the blood.

After a stabilization period of 20-30 min on the CMV ventilator, an arterial blood sample was drawn for blood gas analysis and baseline measurement of tracer gas concentrations. The valve attached to the ventilator pistons was then switched at

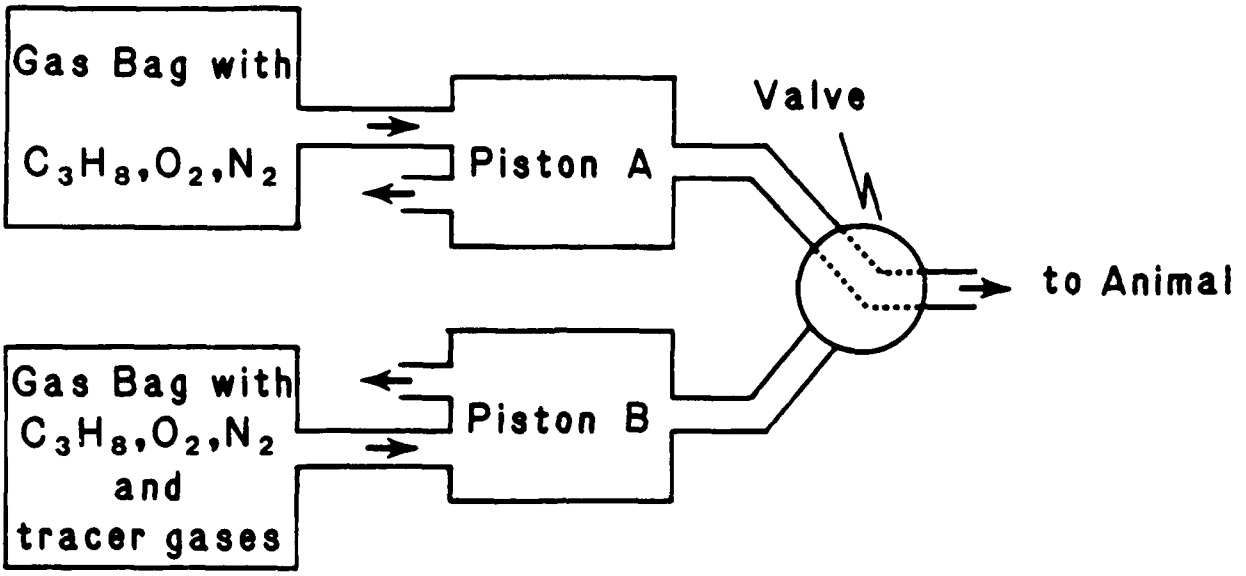

Figure 2. Ventilator circuit used for washin during CMV.

TABLE 1. TRACER GASES

Gas	MW	$(MW^{-1/2})$	Relative Diffusivity	Percentage In Mixture
H_2	2.0	.707	8.55	1.65
He	4.0	.500	6.04	4.92
CH_4	16.0	.250	3.02	.62
C_2H_6	30.1	.182	2.20	.17
C_4H_{10}	58.1	.131	1.59	.12
SF_6	146.1	.083	1.00	.01

MW = molecular weight

end-expiration with the subsequent washin of tracer gases. Arterial blood sampling was initiated at 12, 24, 36, 48, 60, 90, 180, and 240 s after the start of the washin. The time of initiation and completion of each 10 ml sample was noted with an event marker on a strip chart recorder; the midpoint of the sampling period was utilized for subsequent data analysis.

After completing the CMV washin, the animal was transferred to HFV for a similar washin of tracer gases after a 20 min stabilization period. Tidal volume was set at 3 ml/kg; respiratory frequency was maintained at 20 Hz. A specially constructed high-frequency oscillator was used in these experiments (Fig. 3).

The oscillator consisted of a 2.5 in. (6.35 cm) ID Teflon piston within a brass cylinder. A threaded Plexiglas head, with an O-ring seal, was attached to the end of the cylinder and tapered down to a 0.5 in. (1.27 cm) ID outlet. The drive shaft of the piston was driven by a Dayton 1/4 hp motor, with speed adjustable to 1725 RPM (0-28 Hz) by a solid state controller. Stroke volumes up to 100 cc, representing a piston displacement of 0-3 cm, were achieved by adjusting the position of the drive shaft on a motor-driven cam.

A small, flexible gas bag closed the rear of the piston, since preliminary experiments indicated that small amounts of tracer gas could escape between the Teflon piston and the brass cylinder despite closely machined tolerances. Bias flow was

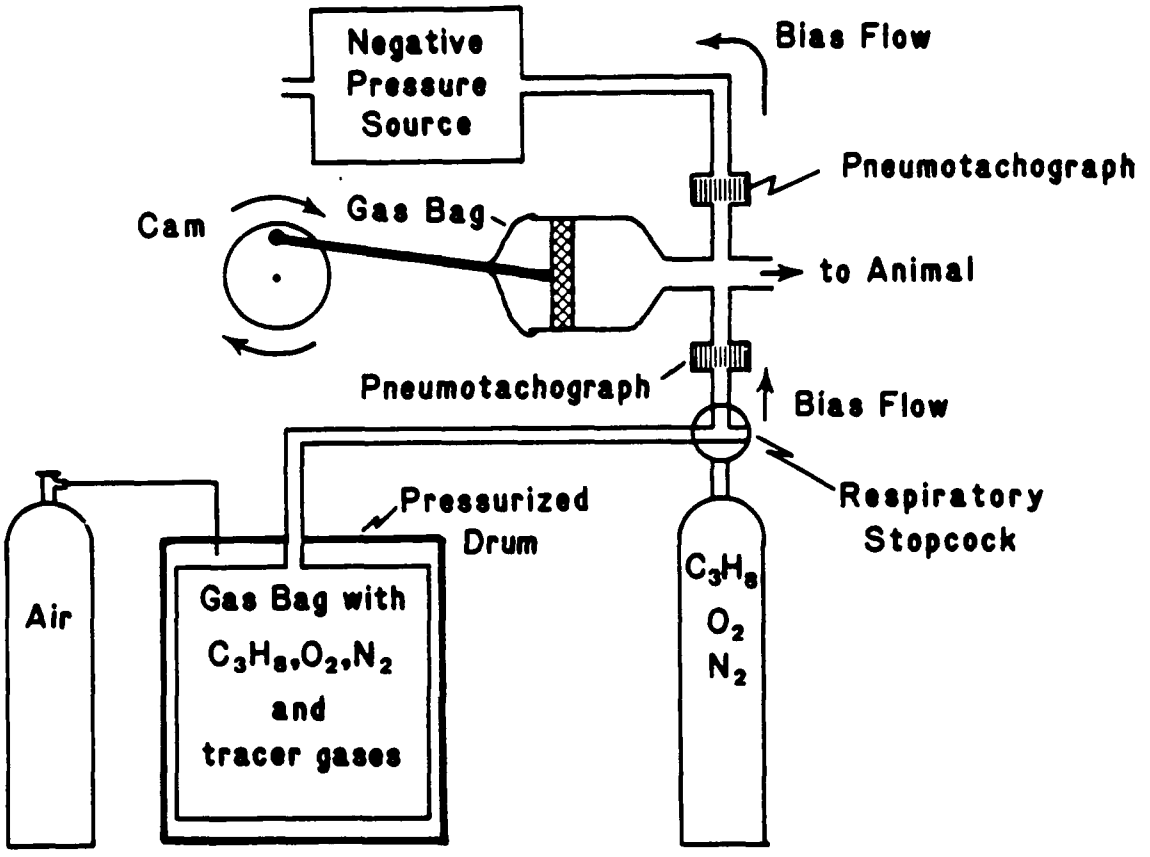

Figure 3. Oscillator circuit used for washin during HFV.

---

introduced into, and removed from, the port of the oscillator through high impedance connections to reduce loss of the tidal stroke through the bias system (5). Fleisch pneumotachographs (#00) and Validyne MP-45 ($\pm$ 2 cm H_2O) transducers were used to measure mean bias flow and fluctuations in bias flow resulting from the ventilatory oscillations in both the inflow and outflow tubing. The pneumotachographs were calibrated using constant flows from a gas cylinder. Flows were measured with a 9 L

water-filled spirometer (Warren E. Collins, Inc.). Less than 5% of the stroke volume of the oscillator was lost through the bias flow pathway. This volume loss is not reflected in the tidal volumes contained in Table 2 since the pneumotachograph utilized for these measurements was placed between the bias flow and endotracheal tube. Gas lost through the bias flow pathway was not measured by this pneumotachograph. To maintain reasonable airway pressures in the face of the high impedance bias flow stream, it was necessary to utilize both a positive pressure source in the entering bias flow and a negative pressure source in the bias flow leaving the system. The negative pressure source was a high-capacity vacuum cleaner with a variable sized leak which enabled adjustment of the applied negative pressure. The propane, oxygen, and nitrogen mixture was supplied to the positive side of the bias flow from a standard high pressure cylinder. The presence of flammable and explosive gases in the tracer mixture precluded use of a standard pre-mixed high-pressure gas cylinder for the washin portion of the experiment. Therefore, a tracer mixture prepared as described above was placed in a gas bag inside a 30-gal (114 L) drum. Using a compressed air tank, the drum was pressurized to the same pressure as the setting on the second stage of the C_3H_8-O_2-N_2 tank regulator. With this system the bias flow could be rapidly changed by turning the respiratory stopcock (Fig. 3) from the gas mixture in the cylinder to the tracer mix in the drum with

minimal interruption of bias flow. The deadspace in the stopcock, bias inflow pneumotachograph and tubing was 65 ml. At the mean bias flow of 6.5 L/min, this deadspace caused a minimal delay in introducing the tracer mixture into the oscillating column. Arterial blood sampling during tracer washin was accomplished in the same manner as in the CMV portion of the experiment. Blood loss due to sampling was replaced with normal saline after each set of samples was collected. At the conclusion of the experiment the animal was euthanatized with a rapid intravenous injection of a saturated KCl solution.

Data were recorded both on an 8-channel strip chart recorder (Model 2800S, Gould, Inc.), and an 8-channel FM tape recorder (Model 3968A, Hewlett Packard, Inc.). Variables recorded included systemic arterial blood pressure, event marks signaling the onset and completion of each arterial sample, mean airway pressure, airflow at the proximal end of the endotracheal tube, bias inflow and outflow, and CO_2 concentration at the connection between the pneumotachograph and the ventilator. Following completion of the experiment, the FM tape was replayed and the signals digitized by a 16-bit analog-to-digital converter in a computer (Kaypro Model 4885) and stored on floppy disc. Data were sampled at 5-ms intervals in the CMV experiments and at 2-ms intervals in the HFV experiments. Heart rate and systolic, diastolic, and mean blood pressures were obtained from the blood pressure recording. Mean airway pressure was obtained from the

electrically filtered signal of airway pressure. Ventilator rate and tidal volume were calculated from the airway pneumotachograph. Volume was obtained by numeric integration of the pneumotachograph output. Bias flow and variations in this flow were obtained from the bias flow pneumotachograph recordings.

Arterial blood pH, Pco_2, and Po_2 were measured with a Radiometer blood gas analyzer (Model MK2) at 37°C. Plasma bicarbonate concentrations were calculated from pH and Pco_2 measurements. Hematocrit was determined by centrifugation of capillary tubes. Hemoglobin was measured with the cyanmethemoglobin technique.

Inert gas concentrations in the blood were measured with a variation of the method of Wagner et al. (6). With this technique an equal volume of inert gas (nitrogen in the present experiments) is added to blood in the sampling syringe. The syringe is agitated in a 37°C water bath until equilibration is reached between the gaseous and aqueous phases. The gaseous phase is removed in a separate syringe and stored for subsequent analysis by gas chromatography. Usually concentrations of the inert gases in the blood are calculated using appropriate solubility coefficients and the relative volumes of the gas and aqueous phases. Blood volume is obtained by weighing the syringes before and after sample collection and calculating blood volume using an assumed density. The volume estimates in these

calculations introduce errors into the measurements and are tedious when a large number of samples are required.

To avoid these problems, all calculations of gas concentrations in the blood were referenced to an internal standard. Inspired gas prior to, and during, washin contained 0.1% propane. Arterial blood was in equilibrium with this gas concentration throughout the washin. Measurements of changing inert tracer gas concentrations were always expressed as a fraction of the constant propane value. The constancy of C_3H_8 provided an internal standard of reference. If errors were made in the blood volume in the sample syringe or in the quantity of nitrogen added to the sample, the absolute amount of tracer gases would vary but their relation to the propane would remain constant. Dilution or relative concentration of a sample would affect all gases equally, and therefore, the tracer gas/propane ratio would remain unchanged. Attainment of a constant tracer gas/propane ratio indicated completion of the washin for the gas in question. This method of analysis implicitly assumes that the propane and tracer gases are all transported in the blood in an identical fashion. Obviously, differing solubility characteristics of the gases violate this assumption, but the highly insoluble nature of the gases utilized as tracers sharply reduces the effect of variations in solubility.

After extraction of the tracer gases into the nitrogen above the arterial blood samples, the gas phase was injected into three

constant volume sampling loops (Fig. 4A) using a series of stopcocks. By switching the individual valves (Fig. 4B), an aliquot of the gas sample was swept into each of three gas chromatographic systems. Valve I was purged with a mixture of 5% methane in argon through an 8-ft column packed with 5A molecular sieve (Matheson Company, Inc.) and maintained at 15°C. The gases eluted from the column passed through an electron capture detector with a scandium source (Analog Technology Corporation) which detected sulfur hexafluoride. Valve II was flushed with helium which carried the sample through a 12-ft column of Porasil B (Waters Associates, Inc.) maintained at 50°C to a flame ionization detector (Model GC 72-5, Beckman Instruments, Inc.) to detect the flammable organic gases. Valve III was flushed with nitrogen through a 6-ft column of activated charcoal (Analabs, Inc.) into a thermal conductivity detector (Model 100, Carle Instruments, Inc.) to detect hydrogen and helium. The column and detector were maintained at 27°C in a waterbath. Chromatographic outputs were recorded on a four-pen chart recorder (Model SC284, Gould, Inc.); gas concentration was expressed in arbitrary units of peak height.

For comparison of variables listed in Table 2 we used analysis of variance with repeated measures design. The statistical model was

$$x_{i,j,m} = \mu + A_i + B_j + \delta_m + A\delta_{i,m} + \epsilon_{i,j,m} \qquad (1)$$

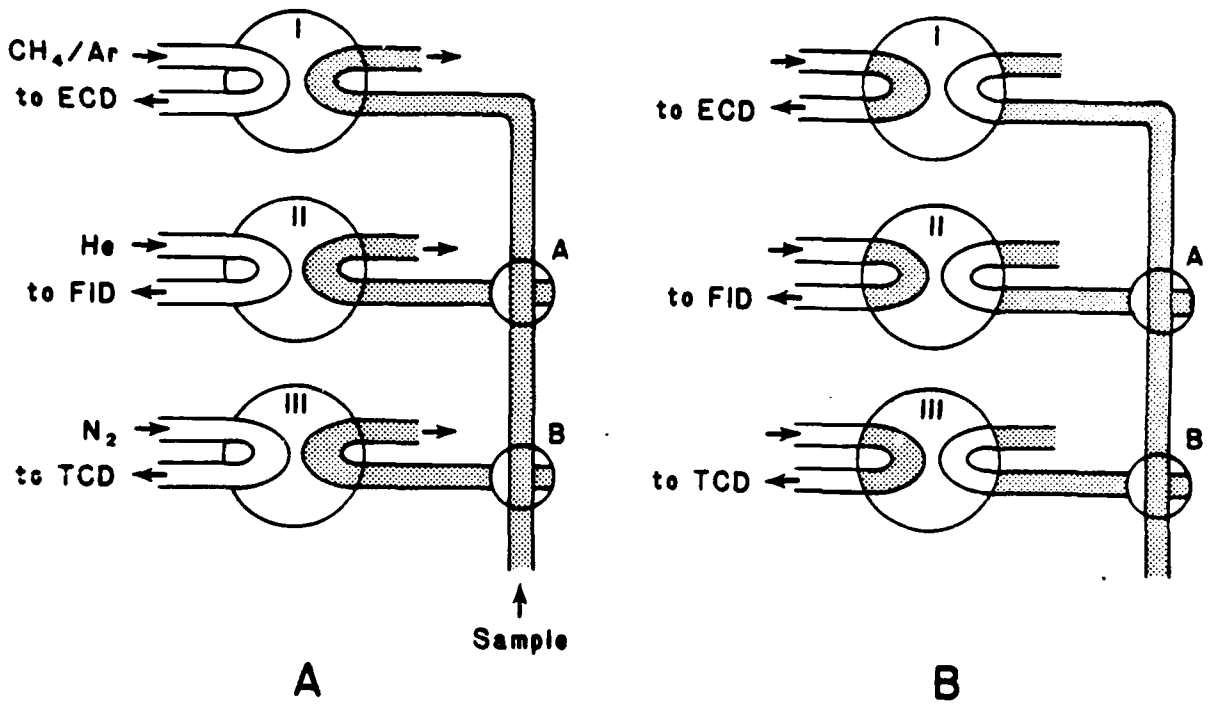

Figure 4. Valve assembly used in measurements of inert gases. Stopcocks labelled A and B permitted filling valves I, II, and III. As shown in the figure, the stopcocks are arranged to fill valve I. A: Valves open to exterior circuit for filling with gas samples (shaded area). B: Valves rotated to admit fixed volume samples into the chromatographic systems. ECD = electron capture detector; FID = flame ionization detector; TCD = thermal conductivity detector.

---

where x is the variable being tested, μ is the mean, A is an effect due to differences between dogs, B is an effect due to differences between pairs of measurements of normal and high-frequency ventilation within the dogs, and δ is an effect due to differences caused by the type of ventilation (CMV or HFV).

$A\delta$ is an effect due to an interaction between A and δ effects and is the experimental error term used to test the effect of different types of ventilation. The term ϵ is the residual sampling error. Subscript i denotes the dog (1 to 5), subscript j denotes the particular pair of measurements (1 to 13), and m denotes the type of ventilation (1 or 2).

Eight measurements of inert gas concentrations in the blood were made at intervals after ventilation with the gas mixture containing the six tracer gases. The sampling schedule was determined from pilot experiments to provide an optimal description of the time course. For each trial, the data were fitted to a first order exponential expression by the least squares criterion for each of the six test gases. To determine if there was a relation between $k_{G_{i,j,m,n}}$, the gas washin rate constant, and the square root of the reciprocal of the molecular weight of each gas $(MW^{-1/2})_n$, we used analysis of covariance with the statistical model

$$k_{G_{i,j,m,n}} = \mu + A_i + B_j + \delta_m + A\delta_{i,m} + \beta(MW^{-1/2})_{m,n} + \epsilon_{i,j,m,n} \quad (2)$$

where β represent the regression coefficients that describe the relation between k_G and $(MW^{-1/2})$ for CMV and HFV. The six inert tracer gases are represented by the subscript n. The rest of the notation is the same as described above. The residual error was used to test the significance of the regression coefficients.

Results

A total of 13 pairs of washin experiments were conducted in five dogs; each pair included a CMV and an HFV washin. The physiological variables measured during these experiments are shown in Table 2 with indices of variation. There were no significant differences in arterial blood gases, hematologic variables or airway pressure between the CMV and HFV experiments. Heart rate was slightly lower in the control animals. Obviously, differences were present in the frequency and depth of respiration ($p < .001$) resulting from the design of the experimental protocol.

The washin of tracer gases with time during CMV and HFV in a representative pair of experiments is shown in Figs. 5 and 6. In these figures, changing gas concentrations are expressed as a fraction of the steady state value of the particular gas.

The data for each gas from each washin were analyzed separately as a single exponential function

$$R_G = R_{G_\infty}\left[1 - e^{-k_G(t-d_G)}\right] \qquad (3)$$

where R_G is the observed ratio of the gas in question (represented by G) to the simultaneous propane value, R_{G_∞} is the ratio at infinite time, k_G is the rate constant describing the kinetics of the washin, t is the time interval following the change of the inspiratory gas mixture, and d_G is a constant

TABLE 2. EXPERIMENTAL VARIABLES: PART I

	CMV		HFV	
	Mean	± S.D.	Mean	± S.D.
pH	7.32	.04	7.32	.03
Pco_2 (mmHg)	39.7	3.2	39.0	4.0
Po_2 (mmHg)	108	13	108	12
$[HCO_3^-]$(mEq/L)	20.3	1.8	19.8	1.6
[Hb](g/dl)	12.7	2.0	12.5	2.5
Hct (%)	38.3	5.1	37.9	5.5
HR (beats/min)	142[a]	19	156	21
$P_{Air,Mean}$ (cm H_2O)	3.5	1.5	6.3	3.2
f (breaths/min)	21.7[a]	3.4	1255.6	13.5
V_T (cc_{BTPS})	315.0[a]	18.4	63.0	3.7
Bias Flow (L/min)			6.5	2.5
BP (mmHg)	160/120	6/8	164/112	12/16

Hct = hematocrit; $P_{Air,Mean}$ = mean airway pressure; f = respiratory frequency; V_T = tidal volume; BP = blood pressure.

[a]significantly different from HFV value ($p < .001$).

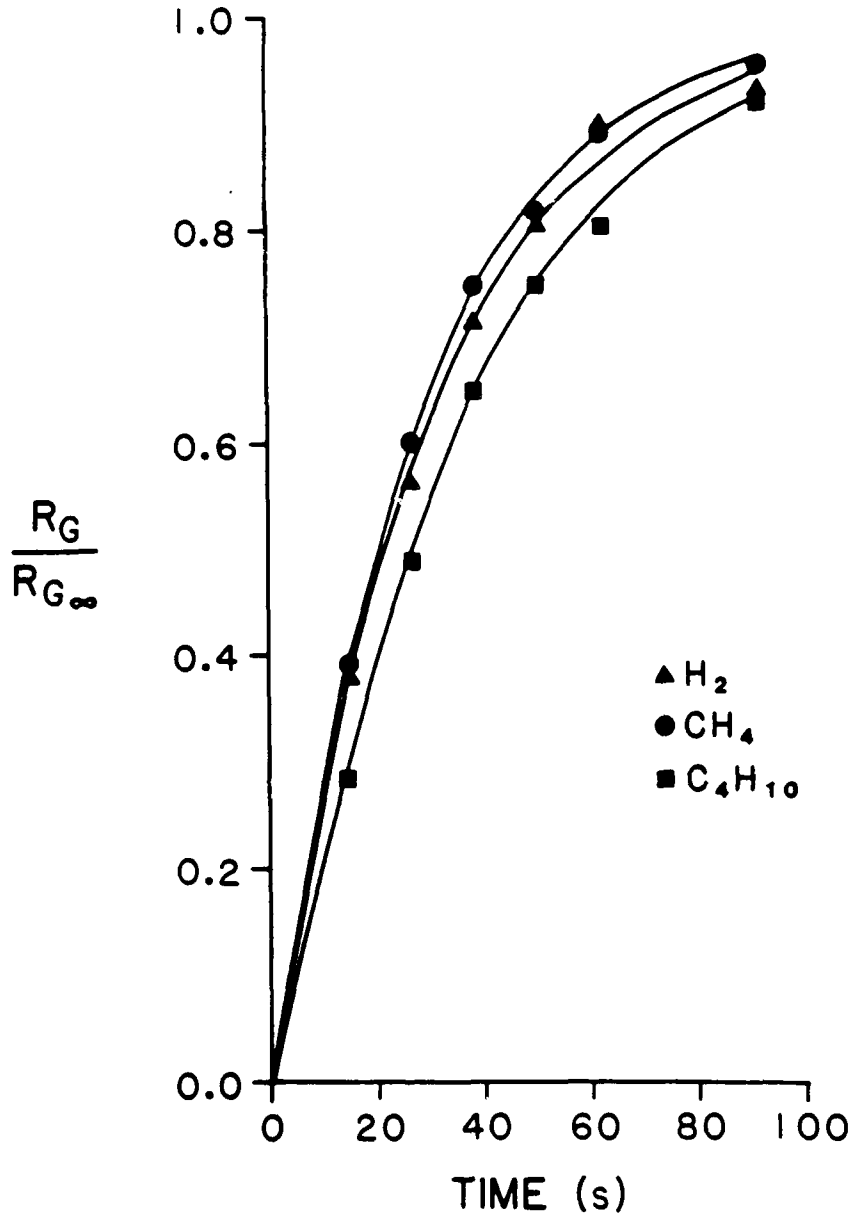

Figure 5. Gas concentrations in experiment 1A during washin with CMV. R_G = gas/propane ratio; $R_{G\infty}$ = gas/propane ratio at infinite time. For clarity, only hydrogen, methane and isobutane data are plotted. Helium, ethane and sulfur hexafluoride data occupy intermediate positions on the graph.

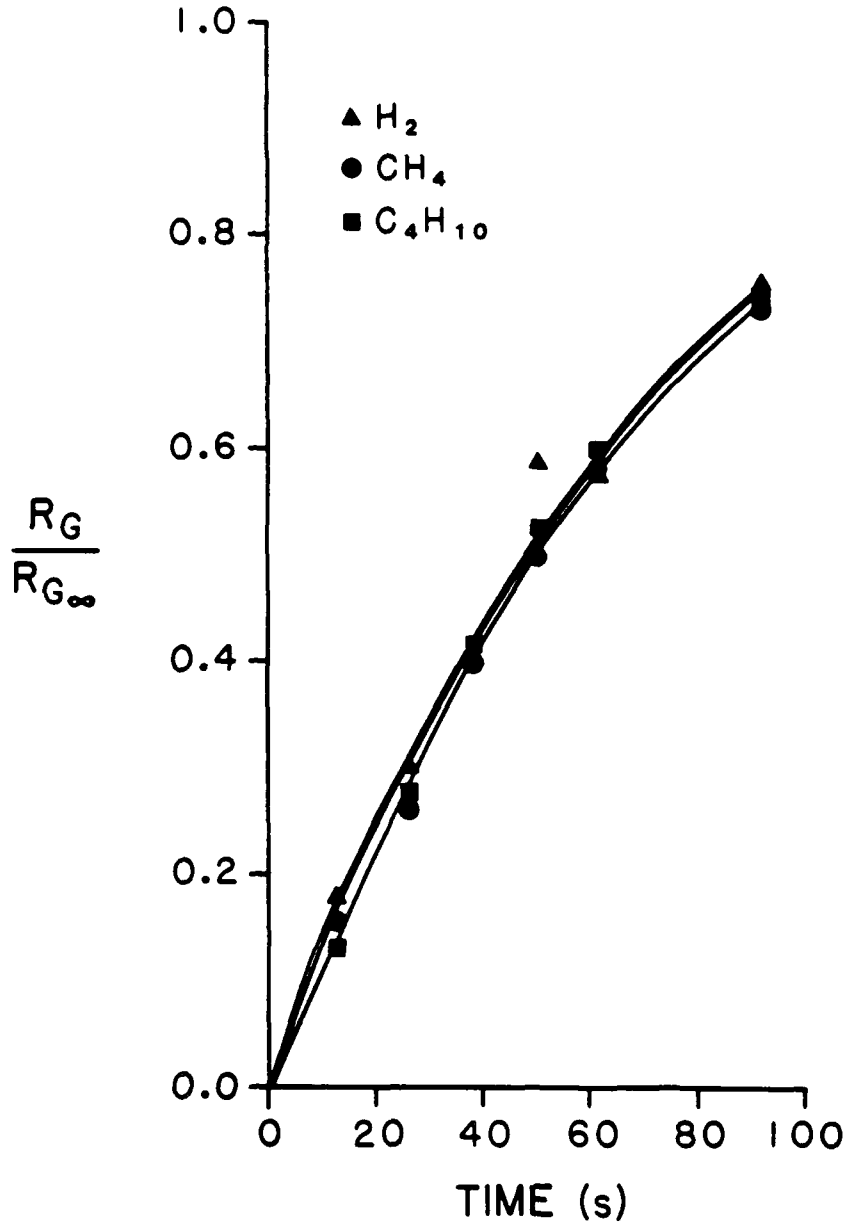

Figure 6. Gas concentrations in experiment 1B during washin with HFV. R_G = gas/propane ratio; $R_{G\infty}$ = gas/propane ratio at infinite time. For clarity only hydrogen, methane and isobutane data are plotted. Helium, ethane and sulfur hexafluoride data would be superimposed on the plotted data.

which reflects the time delay resulting from gas flow through the tracheobronchial tree and blood transit to the aorta. The R_G and t measurements were obtained from experimental observations, and the constants R_{G_∞}, k_G, and d_G were computed simultaneously using the Newton-Raphson technique to minimize the residual sum of squares. The resulting curves are plotted with the experimental data in Figs. 5 and 6. Gas washin was analyzed as a single exponential function because adding a second exponential did not significantly affect the residual sum of squares obtained in the fitting procedure. The effect of molecular weight is better visualized when the curves obtained from equation (3) are plotted in logarithmic format (Figs. 7 and 8). It is apparent that the dispersion of gases during washin is much greater during CMV than the dispersion with HFV.

The mean rate constants and their variations for each gas in the CMV and HFV experiments are listed in Table 3. The rate constants are plotted in Fig. 9 as a function of the inverse of the square root of molecular weight. This latter variable provides a reasonable approximation of the relative diffusivity of each gas (Table 1). The equations of the straight lines fitted to the data plotted in Fig. 9 are listed in the legend to the figure. The slope of the relation of the rate constants to the relative diffusivity in the CMV experiments (β in Table 3) is significantly different from zero ($p < .0001$) as is apparent from Fig. 9. Although the slope of the HFV relation is markedly

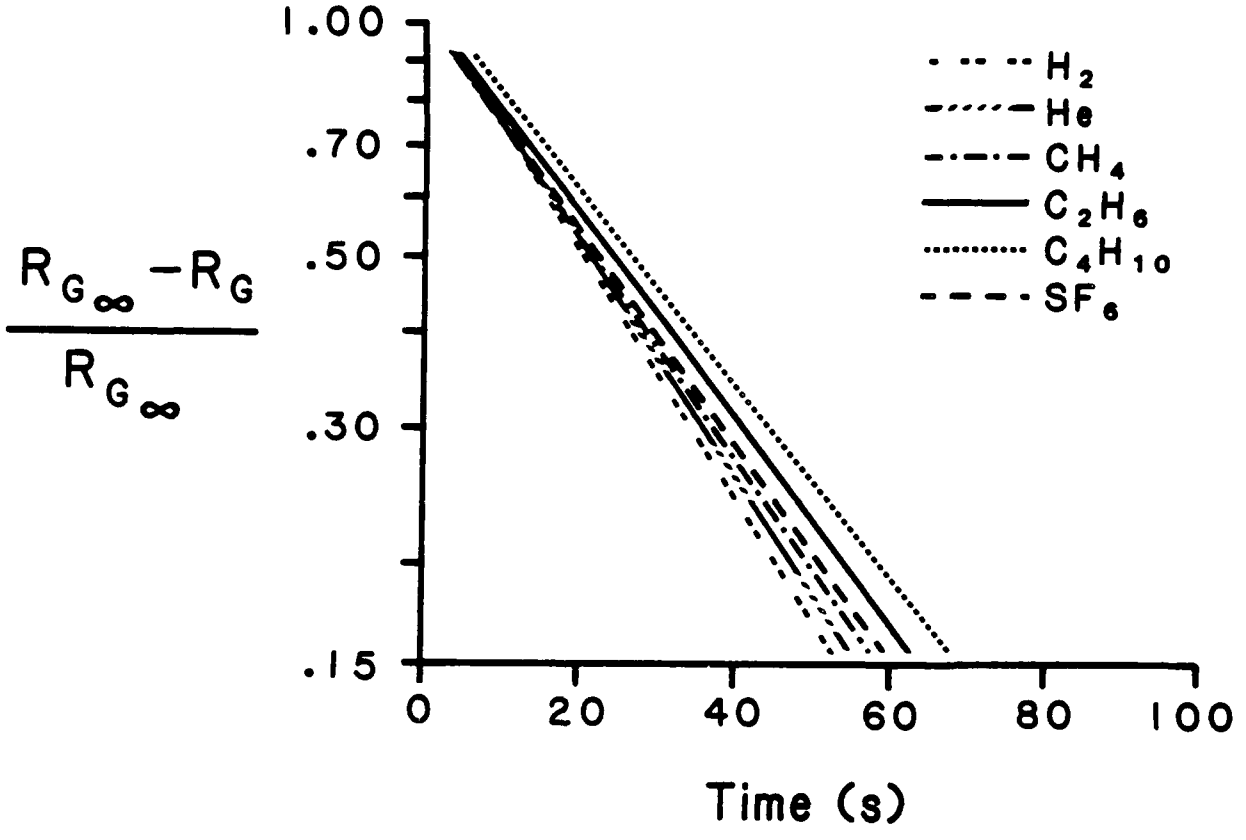

Figure 7. Logarithmic plot of fitted exponential relationships for inert gas washin data from experiment 1A conducted with CMV. R_G = gas/propane ratio; R_{G_∞} = gas/propane ratio at infinite time.

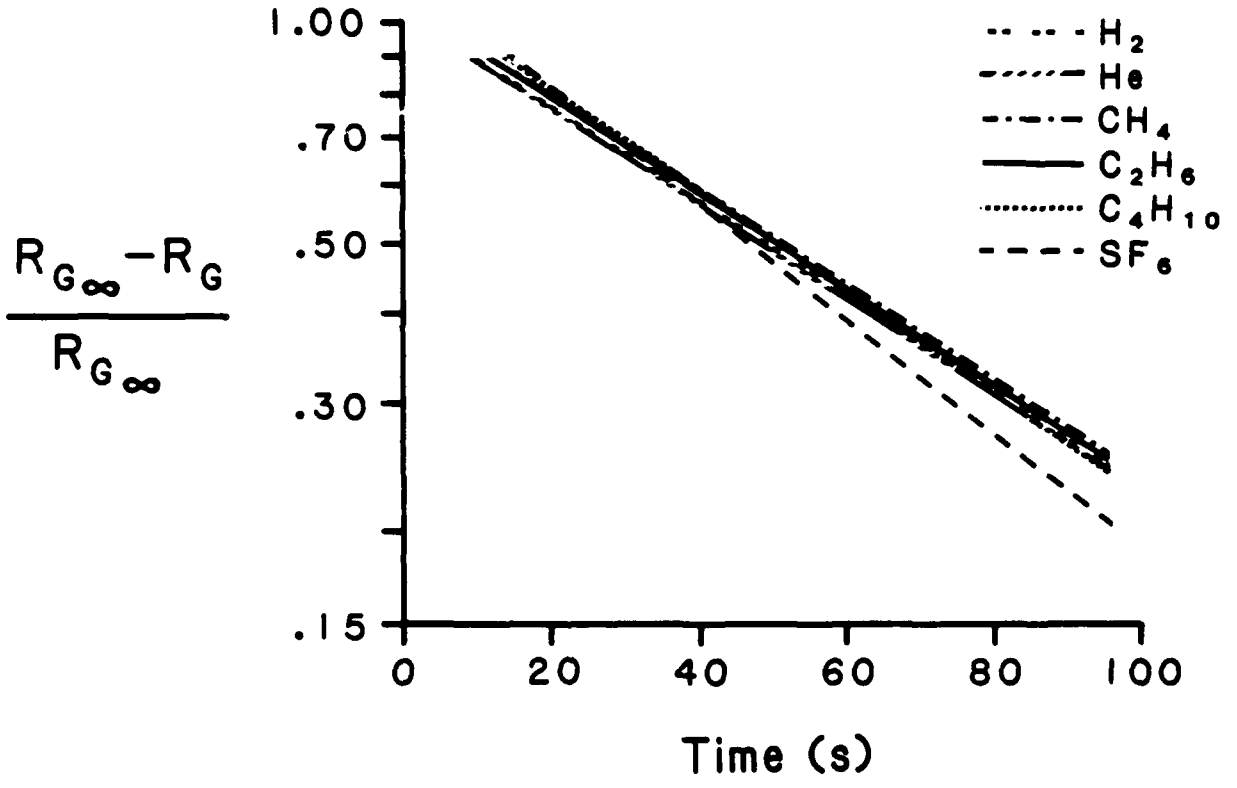

Figure 8. Logarithmic plot of fitted exponential relationships for inert gas washin data from experiment 1B conducted with HFV. R_G = gas/propane ratio; $R_{G\infty}$ = gas/propane ratio at infinite time.

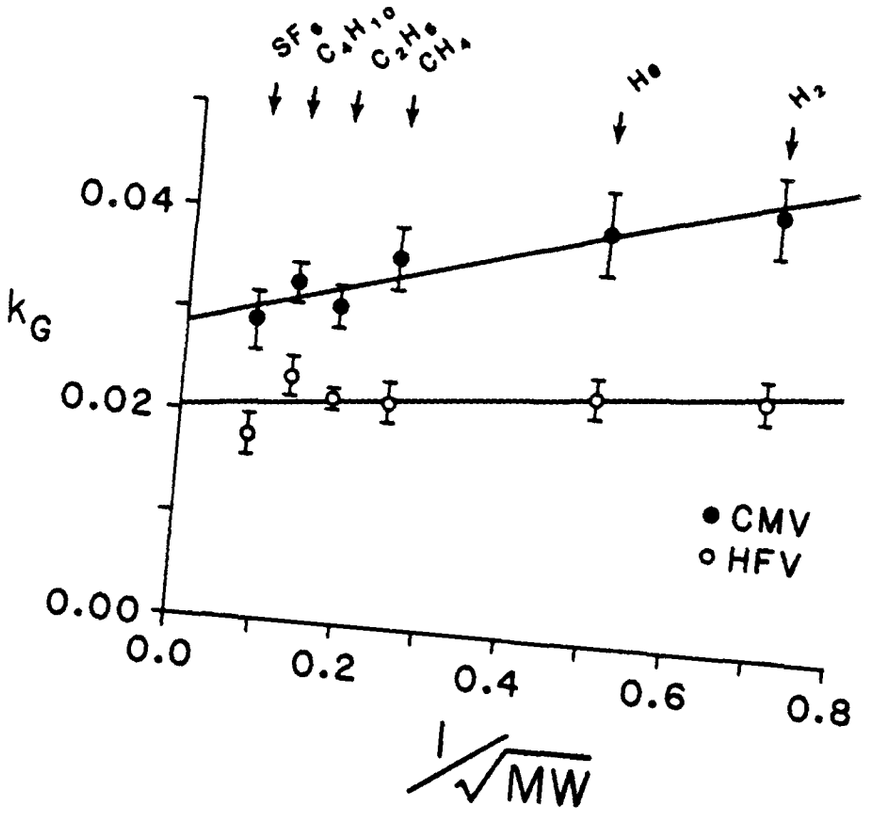

Figure 9. Relationship between the rate constants fitted to the gas washin data and the inverse square roots of the molecular weights of the gases. Filled circles are data obtained during CMV. The equation fitted to the CMV data is [$k_G = 0.0218(MW^{-1/2}) + 0.0286$]. Open circles represent experimental data obtained during HFV. The equation fitted to the HFV data is [$k_G = 0.0069(MW^{-1/2}) + 0.0206$]. Error bars represent ± 1 standard error.

TABLE 3. RATE CONSTANTS FOR GAS WASHIN

k_G (s^{-1})	CMV		HFV	
	Mean	± S.D.	Mean	± S.D.
k_{H_2}	.043	.015	.025	.007
k_{He}	.040	.014	.024	.008
k_{CH_4}	.036	.011	.023	.006
$k_{C_2H_6}$	.031	.007	.023	.005
$k_{C_4H_{10}}$	.033	.008	.024	.006
k_{SF_6}	.029	.010	.018	.006
β[a]	.0218[b]	.0029[c]	.0069[d]	.0020[c]

[a] β is the coefficient from the analysis of covariance [Equation (2)]

[b] Slope significantly different from zero ($p < .0001$) and greater than the HFV slope ($p < .002$)

[c] Standard error of the estimate

[d] Slope significantly different from zero ($p < .001$)

---

different from the CMV data ($p < .002$), its value also is different from zero ($p < .001$) which indicates that diffusion does play a role, albeit small, in gas transfer during HFV.

EXPERIMENTAL STUDY: PART II

Methods

Ten male mongrel dogs were used for these experiments. The animals were premedicated with 4% thiamylal (6 mg/kg) given by rapid intravenous bolus injection. Anesthesia was induced and maintained with α-chloralose in sodium tetraborate buffer. The α-chloralose solution was initially given by intravenous bolus (120 mg/kg), and then followed by a continuous infusion of 43 mg/kg/h. A constant infusion pump was used to maintain accuracy. Muscle paralysis was achieved through repeated intravenous injections of pancuronium bromide. An initial dose of 0.1 mg/kg was given and supplemental doses of 0.04 ml/kg were administered as needed. No data were collected for at least 10 min after an injection of pancuronium bromide. Each dog was intubated with a cuffed No. 10 oral endotracheal tube, and ventilated with a high-frequency ventilator. The oscillator described in Part I of this report was also used for these experiments.

A bias flow supplied inspired gas and allowed for CO_2 washout. Bias flow was measured using a pneumotachograph in the inspiratory bias flow line (Fig. 10). The flow was adjusted to produce a slight positive pressure in the airway before the HFV was turned on. The expiratory bias flow passed through 3-6 ft (.9-1.8 m) of 1/4-in. (6.4 mm) ID Tygon tubing which produced a

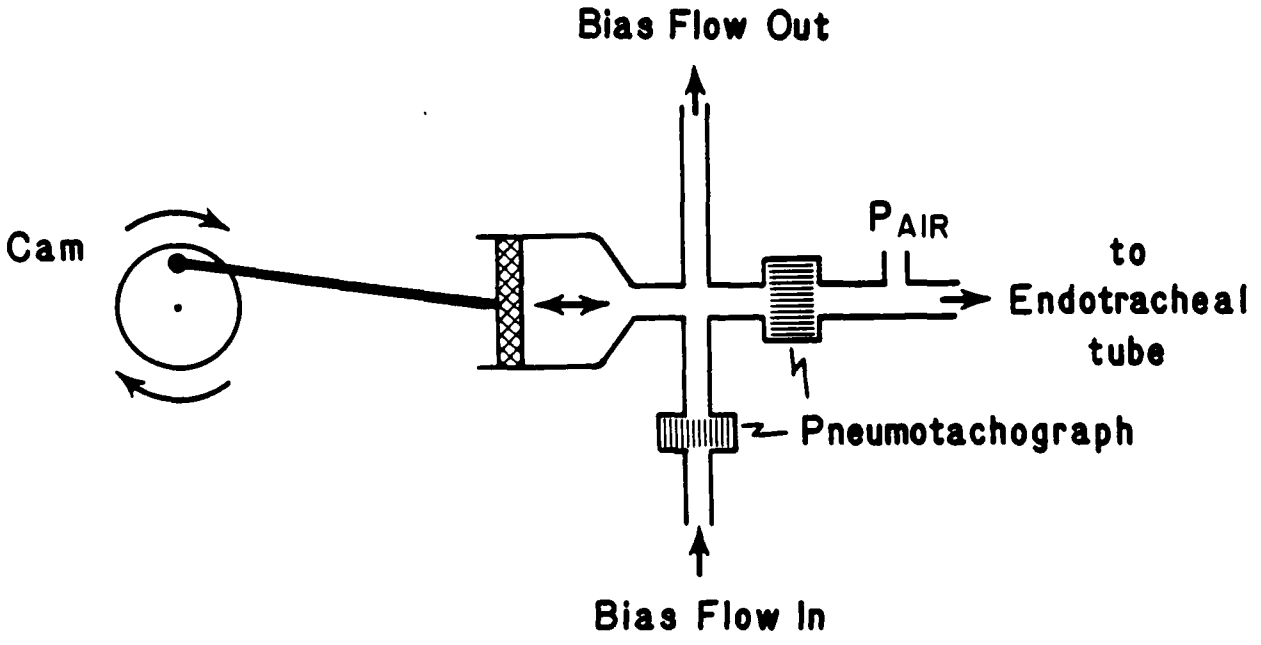

Figure 10. Circuit used for HFV at ground level and at altitude. P_{Air} = airway pressure transducer.

---

relatively high impedance. Control dogs received 21% oxygen via the bias flow, while the oleic acid animals received 100% oxygen. Since the severity of the oleic acid-induced injury varied among animals, an F_IO_2 of 1.0 for the bias flow was chosen to ensure an acceptable arterial Po_2 in all animals. Initial piston stroke volume was set at approximately 3 ml/kg with a respiratory rate of 20 Hz. Adjustments in ventilator stroke volume were made prior to data collection to ensure

eucapneic conditions as determined by arterial blood gas analysis. No further adjustments were made in ventilator settings.

The dogs were instrumented with a jugular venous catheter for fluid and drug administration and with a femoral arterial catheter to monitor blood pressure and collect arterial blood samples. A heating blanket was used to maintain body temperature. A triple lumen Swan-Ganz thermodilution catheter was placed in the pulmonary artery via a femoral vein to collect mixed venous blood samples and to measure pulmonary arterial and pulmonary capillary wedge pressures. Body temperature was monitored by the thermistor located at the tip of the Swan-Ganz catheter.

The oleic acid model of acute respiratory distress syndrome (ARDS) was induced in 5 of the 10 dogs by injecting oleic acid, 0.1 ml/kg, infused into the right atrium via the Swan-Ganz catheter at 0.4 ml/min. The dogs were allowed to breathe spontaneously from a reservoir containing 100% oxygen. Arterial blood gases were monitored and, if needed, the animal was ventilated intermittently with an Ambu bag to prevent severe respiratory acidosis. Approximately 90 min after the oleic acid infusion, the animals were placed on HFV. When blood gases were stable, approximately 2 h after oleic acid infusion, data collection was begun.

Data were recorded with both an 8-channel recorder (Model 2800S, Gould, Inc.) and an 8-channel FM tape recorder (Model 3968A, Hewlett-Packard). The strip-chart recorder was used for on-line monitoring. All calculations were obtained from tape recorder data as described below. The variables recorded were EKG, systemic and pulmonary artery pressures (Model P-23 transducers, Gould, Inc.), pulmonary artery wedge pressure, airway pressure at the proximal end of the endotrachial tube (Validyne MP-45, $\pm$ 50 cm H_2O), bias flow using a Fleisch No. 1 pneumotachograph in the input line, tracheal airflow obtained from a Fleish No. 3 pneumotachograph placed between the bias flow and endotracheal tube, and delivered stroke volume by electrical integration of the pneumotachograph flow signal. Validyne MP-45 ($\pm$ 2 cm H_2O) transducers were used to measure the differential pressure across the pneumotachographs. Arterial and mixed venous blood samples were analyzed at 37°C. Since all animal temperatures ranged between 36 and 38°C, no blood gas corrections for these minor temperature variations were made. Cardiac output was determined using an Edwards thermodilution cardiac output computer. Three to five sequential cardiac output determinations were made using 10-ml injections of saline at room temperature. The cardiac output computer continually monitored the temperature of the injectate solution. Lung volume was estimated by nitrogen dilution using a closed circuit rebreathing technique.

The same data collection protocol was employed for both control and oleic acid animals. After being placed on the HFV, several preliminary arterial blood gases were obtained at 15-20 min intervals. When both arterial Po_2 and Pco_2 were stable, and eucapnia had been achieved, data collection was begun.

The initial data at ground level were collected on two occasions 20-30 min apart and are designated as Ground 1 and 2 conditions. All parameters were measured with each data set except for lung volume, which was determined with the second collection of data. Following data collection, the hypobaric chamber in which the animal was situated was closed and decompressed to a simulated level of 8,000 ft (barometric pressure 564 mmHg). The rate of ascent to, and descent from, 8,000 ft was 2,000-5,000 ft/min. Once altitude was reached, all pressure transducers (airway, systemic and pulmonary artery pressure) were recalibrated. The pneumotachographs were not recalibrated. After a 25-30 min stabilization period, two sets of altitude data (Altitude 1 and 2) were collected using the same protocol as during the ground level conditions. The hypobaric chamber was returned to ground level and, after 25-30 min stabilization, another two sets of measurements (Ground 3 and 4) were obtained. Pressure transducers were recalibrated prior to these measurements. At the conclusion of the experiments, the animals were euthanatized by rapid intravenous injection of a saturated KCl solution.

The data collected on the FM tape recordings were digitized by a 16-bit analog-to-digital converter in a computer (Kaypro Model 4885) and stored on floppy disc. Data from the FM tape recorder were sampled over 20-s periods at a rate of 50 Hz. Mean values for heart rate, airway pressure, pulmonary wedge pressure, and systemic pressure were obtained. Systolic, diastolic, and mean pulmonary arterial pressures also were measured. Ventilator rate and delivered stroke volume were determined from the direct and integrated output of the pneumotachograph. Inspired Po_2 and alveolar Po_2 were calculated, as was the alveolar-arterial Po_2 difference, $(A\text{-}a)O_2$. The cardiac outputs determined with each data set were averaged. Lung volume was calculated from mixing syringe volume and nitrogen dilution data with correction for equipment dead space.

An ANOVA for repeated measures was used for statistical evaluation of the data (7). The experimental design is shown in Table 4. Each variable (arterial oxygen tension, tidal volume, etc.) was analyzed separately. The statistical model used for the analysis was

$$x_{h,i,p} = \mu + \alpha_h + A_i + \eta_p + \alpha\eta_{h,p} + \epsilon_{h,i,p} \qquad (4)$$

where x is the variable being tested, μ is the mean value, α is an effect due to differences between normal dogs and those given oleic acid, A is an effect due to differences among dogs and is used to test the effects of α, η is an effect due to differences

TABLE 4. EXPERIMENTAL DESIGN

	CIRCUMSTANCE											
DOG	GRD 1	GRD 2	ALT 1	ALT 2	GRD 3	GRD 4	GRD 1	GRD 2	ALT 1	ALT 2	GRD 3	GRD 4
Control												
1	x	x	x	x	x	x						
2	x	x	x	x	x	x						
3	x	x	x	x	x	x						
4	x	x	x	x	x	x						
5	x	x	x	x	x	x						
Oleic												
1							x	x	x	x	x	x
2							x	x	x	x	x	x
3							x	x	x	x	x	x
4							x	x	x	x	x	x
5							x	x	x	x	x	x

CIRCUMSTANCE = the condition under which the data was collected.

DOG = the five normal and five oleic acid-treated dogs.

GRD = measurements at ground level. ALT = measurements obtained at altitude. The symbol x signifies when measurements were obtained.

between measurements at ground level before and after altitude simulation, $\alpha\eta$ is an interaction term, and ϵ is the residual term which is used to test the effects of η and $\alpha\eta$. Subscript h represents the group of dogs (normal or oleic acid), i is the particular dog (1 to 10), p denotes whether ground level measurements were made before or after altitude simulation.

To test the effects of altitude and to determine if the effects of altitude are different in the normal and oleic acid treated dogs, we used a similar model:

$$x_{h,i,q} = \mu + \alpha_h + A_i + \lambda_q + \alpha\lambda_{h,q} + \epsilon_{h,i,q} \qquad (5)$$

where λ is an effect due to differences between ground and altitude. The subscript q denotes either ground or altitude, and $\alpha\lambda$ is the interaction term used to determine if the effects of altitude are different between the normal and oleic acid treated dogs. The term ϵ is used to test λ and $\alpha\lambda$. The remaining symbols represent the variables defined above.

Results

A total of 15 mongrel dogs were required for ten successful experiments. Two oleic acid animals died before measurements were completed. In three other experiments, technical difficulties precluded completion of the protocol. Dogs weighed between 13.8 and 19.5 kg. There was no significant difference in the average weight of the 5 dogs used as controls (16.7 kg) when compared with the 5 oleic acid animals (16.5 kg).

Results are summarized in Table 5. Effective alveolar ventilation, indicated by arterial Pco_2, was normal in control and oleic acid animals, and did not change with exposure to altitude. There also was no difference in arterial pH between the two groups, indicating similar acid-base status. Ventilator tidal volume required to produce eucapnea differed in the two groups; tidal volume averaged 60% higher in the oleic acid animals. Respiratory rate was almost identical in both groups, although it was statistically higher in the oleic acid animals. The higher delivered volumes needed to maintain eucapnia in the oleic acid animals indicate that major alterations in gas exchange occurred in the oleic acid animals.

The tidal volume, as judged by the integrated flow signal, decreased significantly with altitude by about 9%. However, some of this decrease may be related to the failure to recalibrate the pneumotachograph at altitude. Tidal volume also decreased over time; tidal volume from Ground 1 and 2 conditions was larger than that seen during Ground 3 and 4. Most of this change over time in tidal volume was attributable to a drop in volumes in the oleic acid group. Most likely this change is secondary to worsening lung function which occurs slowly over time in the oleic acid lung injury model. Ventilation was clearly influenced by respiratory impedance; the increasing impedance in the oleic acid group caused a slight drop in delivered tidal volume. During the final two control periods, accurate tidal volumes

were obtained in only 3 of the 5 oleic acid animals. In the other two experiments, the pneumotachograph became contaminated with pulmonary edema fluid during the final two ground periods, rendering it impossible to accurately integrate flow to calculate tidal volume. The 3 dogs in whom accurate data were obtained at all observations had a mean tidal volume of 77.5 ml during the initial two ground periods; tidal volume fell significantly to a mean of 70.8 ml in the final two ground level conditions. The 2 animals with incomplete data collection had higher initial volumes. This fall in tidal volume had no physiologic importance, since effective ventilation, as judged by arterial Pco_2, was stable under all conditions. Ventilator output, therefore, must have been relatively stable during the course of this study. We conclude that HFV performance was, for all practical purposes, not adversely affected by altitude.

Airway pressure was higher in the oleic acid animals when compared with controls, probably related to a decreased lung compliance secondary to the oleic acid lung injury in this group. An increased resistance to airflow may have also been present, related to the decreased lung volume in the oleic acid animals. Functional residual capacity (FRC) was approximately 75% larger in the controls compared to the oleic acid group ($p < .025$). There was a slight rise in FRC with altitude in the normals, while a fall in FRC with altitude was seen in the oleic acid injured group. FRC returned to its previous baseline in both

TABLE 5. SUMMARY OF RESULTS

Parameter		Group	Ground 1	Ground 2	Altitude 1	Altitude 2	Ground 3	Ground 4
pH_a		Control	7.41 ± 0.07	7.42 ± 0.06	7.40 ± 0.06	7.40 ± 0.06	7.39 ± 0.06	7.39 ± 0.06
		Oleic	7.38 ± 0.03	7.39 ± 0.03	7.39 ± 0.03	7.40 ± 0.03	7.39 ± 0.04	7.38 ± 0.04
P_aCO_2 (mmHg)		Control	37.7 ± 3.7	37.0 ± 3.8	39.2 ± 4.7	39.9 ± 4.2	39.1 ± 6.3	38.7 ± 6.3
		Oleic	40.6 ± 2.9	40.0 ± 4.4	39.5 ± 6.3	37.9 ± 8.6	40.1 ± 7.4	38.6 ± 8.6
Tidal Vol (cc_{BTPS})	a	Control	54.3 ± 10.1	54.6 ± 10.0	51.7 ± 9.4	51.9 ± 9.2	53.3 ± 10.2	53.0 ± 10.1
		Oleic	86.9 ± 21.6	87.2 ± 21.5	81.4 ± 20.8	80.5 ± 21.0	70.6 ± 20.4	70.9 ± 21.3
Resp Rate (Hz)	b	Control	15.3 ± 0.3	15.2 ± 0.6	15.4 ± 0.3	15.5 ± 0.3	15.4 ± 0.4	15.4 ± 0.3
		Oleic	15.8 ± 0.2	15.9 ± 0.2	16.1 ± 0.1	15.9 ± 0.4	15.9 ± 0.3	16.0 ± 0.4
Bias Flow (L/min)	c	Control	12.9 ± 0.9	13.0 ± 0.9	13.2 ± 0.5	13.4 ± 0.3	13.1 ± 0.7	13.2 ± 0.6
		Oleic	14.4 ± 1.6	14.3 ± 1.3	14.4 ± 0.7	14.7 ± 0.7	15.8 ± 1.4	15.5 ± 1.2
$P_{Air,Mean}$ (mmHg)	d	Control	5.6 ± 1.5	5.6 ± 1.5	5.7 ± 1.9	5.9 ± 1.7	6.1 ± 2.0	6.1 ± 1.9
		Oleic	8.5 ± 2.4	8.5 ± 2.4	8.4 ± 2.3	8.9 ± 2.4	10.3 ± 3.2	10.1 ± 3.0
FRC (cc_{BTPS})	e	Control		954 ± 168		1049 ± 402		952 ± 254
		Oleic		608 ± 241		490 ± 189		581 ± 125
Heart Rate (beats/min)	f	Control	124 ± 29	120 ± 25	108 ± 22	102 ± 23	101 ± 23	94 ± 18
		Oleic	140 ± 53	133 ± 53	119 ± 49	122 ± 52	135 ± 54	130 ± 52
Q (L/min)	g	Control	2.7 ± 0.8	2.6 ± 0.7	2.6 ± 0.5	2.5 ± 0.5	2.4 ± 0.5	2.3 ± 0.5
		Oleic	1.7 ± 0.7	1.6 ± 0.6	1.7 ± 0.4	1.7 ± 0.3	1.7 ± 0.4	1.7 ± 0.4
$P_{Art,Mean}$ (mmHg)	h	Control	104 ± 11	107 ± 12	111 ± 13	113 ± 11	110 ± 11	116 ± 8
		Oleic	134 ± 19	134 ± 19	134 ± 16	134 ± 22	129 ± 13	127 ± 12
$P_{Pulm,Mean}$ (mmHg)	i	Control	19.2 ± 7.6	19.1 ± 7.2	24.1 ± 8.4	24.6 ± 8.5	20.3 ± 7.6	20.9 ± 7.0
		Oleic	28.1 ± 14.7	30.1 ± 16.2	27.7 ± 14.0	30.1 ± 15.8	31.5 ± 15.1	33.2 ± 17.0

$P_{Wedge,Mean}$ (mmHg)	j	Control	5.8 ± 3.2	6.3 ± 2.5	4.9 ± 1.9	5.9 ± 2.5	7.5 ± 3.5	7.2 ± 2.6
		Oleic	6.6 ± 3.2	5.7 ± 3.8	2.0 ± 5.8	4.4 ± 6.6	5.5 ± 2.7	5.6 ± 3.4
P_aO_2 (mmHg)	k	Control	98 ± 8	99 ± 7	63 ± 8	63 ± 10	96 ± 9	98 ± 11
		Oleic	176 ± 162	168 ± 148	153 ± 136	161 ± 153	206 ± 202	193 ± 193
P_vO_2 (mmHg)	l	Control	45 ± 4	45 ± 4	39 ± 2	38 ± 2	43 ± 3	43 ± 3
		Oleic	41 ± 5	39 ± 5	35 ± 5	34 ± 5	37 ± 5	36 ± 7
$(A-a)O_2$ (mmHg)	m	Control	3 ± 9	3 ± 7	-1 ± 6	-2 ± 6	4 ± 3	2 ± 6
		Oleic	480 ± 166	489 ± 153	324 ± 139	319 ± 157	450 ± 210	465 ± 201

[a] Tidal Vol
Oleic > Control, p<.05
Ground 1,2 > Ground 3,4, p<.001
Ground > Altitude, p<.001
(See text for explanation)

[b] Resp Rate
Oleic > Control, p<.025

[c] Bias Flow
Oleic > Control, p<.025
Ground 3,4 > Ground 1,2, p<.001

[d] $P_{Air,Mean}$
Oleic > Control, p<.05
Ground 3,4 > Ground 1,2, p<.001

[e] FRC
Control > Oleic, p<.025

[f] Heart Rate
Ground 1,2 > Ground 3,4, p<.01
Ground > Altitude, p<.05

[g] Q
Control > Oleic, p<.05
Ground 1,2 > Ground 3,4, p<.05

[h] $P_{Art,Mean}$
Oleic > Control, p<.05

[i] $P_{Pulm,Mean}$
Ground 3,4 > Ground 1,2, p<.001
Altitude effect for
Control > Oleic, p<.001

[j] $P_{Wedge,Mean}$
Ground > Altitude, p<.025

[k] P_aO_2
Ground > Altitude, p<.001

[l] P_vO_2
Ground > Altitude, p<.001

[m] $(A-a)O_2$
Oleic > Control, p<.01
Ground > Altitude, p<.001
Altitude effect for
Oleic > Control, p<.001

groups on return to ground level. However, these small changes in FRC were not statistically significant.

Heart rate was similar in both groups but cardiac output was lower in the oleic acid group when compared to controls. A decrease in cardiac output after the onset of oleic acid-induced pulmonary edema has been reported by others and is believed to be related to the increase in pulmonary vascular resistance which is seen in this model (8). Mean systemic arterial blood pressure was higher in the oleic acid animals than in the controls. This difference, when combined with the decreased cardiac output noted in the oleic acid dogs, indicates substantial elevation of peripheral vascular resistance in these animals. This finding may have been due to increased neurohumoral activity in this group as a response to the oleic acid injury.

Mean pulmonary artery pressure was higher in the oleic acid group, but this did not reach statistical significance. There was a statistically significant, but clinically irrelevant, increase in the mean pulmonary artery pressure over time. Pulmonary artery pressure rose during altitude exposure in the controls, but not in the oleic acid animals. This finding, which is shown in Fig. 11, probably represents hypoxic vasoconstriction occurring in the normal animals in response to the lower P_aO_2 seen at altitude. The pulmonary artery pressure increase was not seen in the oleic acid animals, since they received 100% oxygen and were not hypoxemic, even at altitude. Pulmonary artery wedge

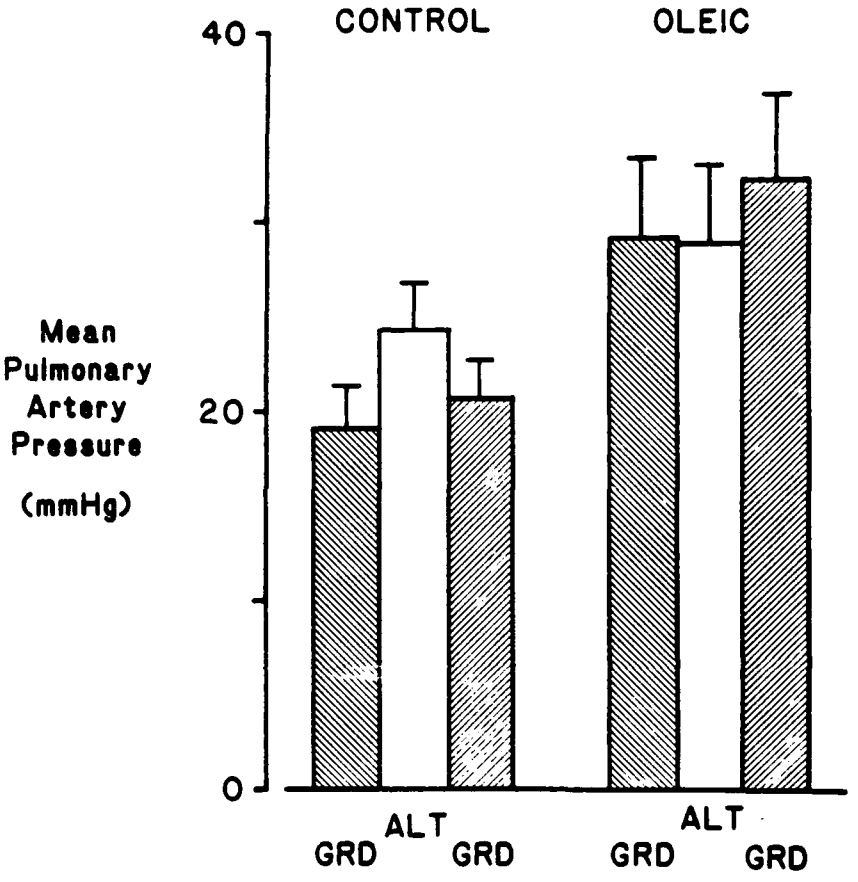

Figure 11. Mean pulmonary artery pressure at ground level and altitude in normal animals and animals with oleic acid-induced lung injury. Error bars represent ± 1 standard error.

pressure was similar in both oleic acid animals and controls, but was lower at altitude than at ground level.

Oxygen exchange was grossly abnormal in the oleic acid injured group. Despite receiving 100% O_2 which resulted in an inspired Po_2 of approximately 700 mmHg at ground level, these

animals had a mean P_aO_2 of 186 mmHg for the four ground level observations. There was a wide range of P_aO_2 in this group, and pre-altitude (Ground 1 and 2) P_aO_2 varied from 68 to 462 mmHg. At 8,000 ft, inspired Po_2 was 521 mmHg and the mean P_aO_2 was 157 mmHg. The mean alveolar-arterial oxygen difference $(A-a)O_2$ of the group was 471 mmHg at ground level (Ground 1-4) and 322 mmHg at altitude (Altitude 1 and 2). This large $(A-a)O_2$ on 100% O_2 is evidence for a large right to left intrapulmonary shunt, as would be expected in a model of lung injury simulating ARDS.

The control group had normal blood gas values under ground level conditions. At 8,000 ft, inspired Po_2 decreased to 108 mmHg from about 147 mmHg under ground conditions. This 39 mmHg decrease in inspired Po_2 resulted in an average decline in arterial Po_2 of 35 mmHg from 98 mmHg (Ground Levels 1 and 2) to a mean of 63 mmHg during the altitude periods.

Mixed venous Po_2 was not significantly different between the control group and the oleic acid group, even though the oleic acid animals all received 100% O_2 and had much higher arterial oxygen tensions. A small but statistically significant decline in P_vO_2 occurred with altitude, resulting from the fall in P_aO_2 in that setting.

DISCUSSION

The existence of molecular diffusion in an axial direction has been demonstrated during normal gas exchange. Power (9) administered a mixture of hydrogen and sulfur hexafluoride to

normal subjects during inspiration. In the subsequent expiration, when the two gases separated, the sulfur hexafluoride concentration was greater initially, but in the terminal portion of the expiratory phase, the relative concentrations were reversed and hydrogen predominated. Power (9) interpreted these observations as evidence for increased diffusive movement of the lighter gas in terminal portions of the tracheobronchial tree during inspiration. The deeper penetration of the gas with greater diffusivity resulted in a relative enrichment of the heavier gas early in the subsequent expiration. The separation of hydrogen and sulfur hexafluoride in these experiments was abolished with a short breath-hold between inspiration and expiration. This observation lends further support to the concept that a time-dependent diffusive process occurs during movement of gas into the alveolar space.

Consideration of the linear velocities of inspired gas in the tracheobronchial tree also supports the concept that molecular diffusion is the dominant process responsible for gas mixing in the distal portions of the tracheobronchial tree. The velocity of gas flow in the trachea is high, but with subsequent branching of airways, the cumulative cross-sectional area of the tracheobronchial tree increases by several orders of magnitude. Accordingly, linear velocity in distal generations drops substantially, and diffusive, rather than convective, movement predominates. With increasing tidal volume, the profile of

inspired gas penetrates deeper into the lung, presumably decreasing the distance between the profile and the alveolar surface. Hence, larger tidal volumes should decrease dependence upon diffusive movement. This reasoning suggests that diffusive processes would be even more important during HFV with small tidal volumes. However, the high frequencies utilized with this mode of ventilation result in peak velocities which are much greater than those seen with conventional ventilation. Even though the tidal volume is smaller by a factor of 5 to 10 with HFV, the respiratory frequency is 50-100 times greater. Thus, linear velocity is much greater and may offset disadvantages in gas movement resulting from the small tidal volumes.

The demonstration of diffusion-dependent processes in the lung does not necessarily indicate that these processes limit overall gas exchange. Recently Robertson et al. (10) have demonstrated that steady state gas exchange is affected to a minor degree by the diffusive properties of the gases studied. These authors also found no difference in diffusion-dependent exchange during CMV or HFV. They concluded that even though diffusive mixing occurred during ventilation, the net effect of this process on overall gas exchange was minimal.

Intrapulmonary gas mixing, promoted by the rapid oscillations occurring during HFV, may be an important factor. Schmid et al. (11) studied clearance of radioactive xenon during HFV. Injection of the xenon dissolved in saline into the right

atrium resulted in greater concentrations of the gas in lower lung zones, consistent with a gravity-dependent distribution of perfusion. However, HFV resulted in an immediate redistribution of the xenon between lower and upper lung zones, indicating that the oscillatory movement promoted intrapulmonary gas mixing.

Knopp and co-workers (12) investigated the potential role of diffusive movement during HFV by measuring lung washout of helium and sulfur hexafluoride. They found no evidence of gas separation in these experiments, suggesting that diffusion was not a dominant mechanism in HFV. Unfortunately they did not study CMV in the same experimental protocol so that comparisons between the two modes of ventilation could not be made. The same group later demonstrated a diffusion effect during HFV, utilizing single breath measurements of gas concentrations after varying periods of HFV (13). This effect was small and less than that seen during CMV. They concluded that gas separation due to diffusion did occur but was probably confined to the alveolar level. Gas movement in upper airways was unaffected by diffusion.

Berdine et al. (14) also studied gas washout during HFV. Similar to the findings of Knopp et al. (12), they observed that the first phase of washout of inert gases was dominated by the establishment of gas gradients along central airways. Both groups of investigators used curve-stripping techniques to demonstrate the presence of two or three virtual lung compartments

during HFV. The initial portion of washout reflected changes in proximal airways. The more terminal portions of the washout curves presumably reflected more distal gas profiles. As emphasized by Berdine et al. (14), subtle differences in the terminal phase of the washouts are difficult to detect because the signal-to-noise ratio is low during this period.

Our approach using multiple gases studied during washin has two distinct advantages. First, the use of multiple gases encompassing a wide range of diffusivities provides an effective means to investigate potential effects of Taylor diffusion. If Taylor diffusion is a factor in gas exchange, gases with high diffusivities would leave the convective profile and lag behind heavier gases which remained in the convective stream. If molecular diffusion were dominant downstream, the remaining gases would separate according to diffusivity. This combination of Taylor and molecular diffusion would result in gases with intermediate molecular weights first reaching the alveolar surface, followed by both lighter and heavier gases. The lighter gases would be delayed by the effect of radial (Taylor) diffusion and the heavier gases as a result of molecular diffusion in the axial direction. Multiple probes with a range of diffusivities are necessary to demonstrate these potential mechanisms. The second advantage of our method of studying gas exchange is the use of gas washin, rather than gas washout. The gas washout process is dominated by the establishment of gas gradients in the

central airways (12, 14), making it difficult to discern changes in peripheral airways. With the washin technique, inert gases do not appear in the blood until the central gradients are established. The initial portion of the gas washin reflects events in the distal airways and alveoli. Thus, the large signal-to-noise ratio occurring during the initial portion of the washin permits maximum detection of distal diffusion-dependent processes. This factor permitted fitting of the present experimental data to a single exponential model rather than the multi-exponential approach used by others (12, 14). The simpler model is possible because the confounding effect of the central airway compartment is not present.

The constants of the rate of gas washin were larger in CMV than in HFV (Fig. 9), indicating that the steady state is reached more quickly in CMV. Establishment of gas profiles in the airways is more rapid with large tidal volumes. Our observations of a major effect of molecular weight on gas washin during CMV confirm the previous observation (10) that diffusion-dependent processes are operative in distal lung units during mechanical ventilation. There is a much smaller, but real, effect of gas diffusion in HFV. The slope of the relation between washin and diffusivity is significantly different from zero during HFV (Fig. 9). However, the role of diffusion during HFV is much smaller than that seen with CMV.

Rates of gas washin demonstrate a progressive effect of molecular weight. The linear increase in the rate constants with relative diffusivity effectively eliminates the possibility that Taylor diffusion plays a significant role in exchange. This finding supports theoretical studies of gas exchange (15) which conclude that Taylor diffusion is not important in HFV because gas diffusivities fall outside of the ranges which are necessary for this process to exert an effect.

Our data indicate an increasing effect of molecular weight on gas washin, a finding which was not present in the washout experiments of Knopp et al. (12). This effect was small, but definitely present in our data. Most likely the failure to demonstrate a molecular weight effect during HFV in previous work (12) is the result of the decreased sensitivity of washout experiments to detect subtle processes occurring deep within the lungs.

The purpose of Part II of this study was to determine whether a high-frequency ventilator would perform adequately, under both ground and hypobaric conditions, and therefore meet the ventilatory requirements of an experimental model of ARDS. This information is crucial if HFV is to be used in clincal situations at altitude. The data from this study can be used as a guide to establish criteria for successful aeromedical evacuation of patients with respiratory failure who are ventilated with HFV.

The aeromedical evacuation issue was approached first by evaluating cardiorespiratory and blood gas information obtained from normal, anesthetized, apneic animals ventilated by HFV under ground level conditions and at a simulated altitude of 8,000 ft. This hypobaric condition is similar to that maintained with commercial and military aircraft flying at approximately 40,000 ft. Acute lung injury was induced in a second group of animals by intravenous injection of oleic acid. Oleic acid produces a lung injury similar to that observed in ARDS. These animals received 100% O_2 via a bias flow while on HFV, and the same hemodynamic and blood gas measurements were made in these animals as in the control group.

The use of 100% oxygen in the oleic acid animals was employed for several reasons. First, it ensured an adequate PaO_2 in all animals, even in those with the most severe lung injuries. Second, it imposed a constant total experimental time on all oleic acid animals. Time-related changes would have been more difficult to analyze if a variable period of time had preceded the start of each experiment while F_IO_2 was adjusted to bring PaO_2 to a predetermined, adequate level. Although this is the usual procedure employed in clinical situations, it would have resulted in a different experimental protocol for each animal in our study. This approach was not feasible in our experimental design since scheduling both hypobaric chamber access and chamber crew assignments precluded experimental runs of varying lengths.

A high-frequency ventilator, with tidal volume generated by piston dispacement within a cylinder, was chosen for these experiments. We reasoned that a volume displacement drive would be less subject to changes during simulated altitude than a pressure-driven HFV. A high-frequency jet ventilator system was not evaluated since measurements of tidal volume are extremely difficult when a jet ventilator is employed, requiring the use of a pressure-compensated, integrated-flow body plethysmograph. The accuracy of such a device at the frequencies employed during HFV is debatable.

The fact that arterial Pco_2 did not change during hypobaric conditions indicated that HFV supplied constant effective alveolar ventilation throughout the experiments. Because the mechanisms underlying HFV are poorly understood, the arterial Pco_2 is the only practical means to judge the effectiveness of HFV (8).

These data indicate that as long as the same HFV tidal volume is delivered at altitude as at ground level, no change in arterial Pco_2 or acid-base status will occur. If ventilation, as assessed by arterial Pco_2, is adequate at ground level in HFV patients with respiratory failure, no change in HFV is necessary during aeromedical evacuation. These data suggest that alteration of gas density resulting from exposure to reduced barometric pressure does not affect the efficacy of HFV.

The normal animals exhibited an average drop in arterial Po_2 at 8,000 ft of 35 mmHg, approximately equal to the decrease in inspired Po_2 of 39 mmHg which occurred from ground level to altitude. The control animals also had a significant increase in pulmonary artery pressures when taken to a simulated altitude of 8,000 ft. If inspired Po_2 were increased at altitude to the same value present at ground level, neither the hypoxemia nor the hypoxic pulmonary vasoconstriction should occur. This situation could be achieved by administering 29% O_2 at 8,000 ft, resulting in the same inspired Po_2 (149 mmHg) found at sea level. It is sufficient to administer approximately 30% oxygen during aeromedical evacuation to prevent alteration of physiological parameters in a patient with normal lungs who requires mechanical ventilation, e.g., respiratory failure caused by neuromuscular disease.

The 5 animals with oleic acid-induced lung injury had markedly elevated alveolar-arterial oxygen differences, which indicates the marked abnormalities in gas exchange occurring as a consequence of the diffuse lung injury caused by oleic acid. However, the changes in oxygen tensions with altitude were very much different from that seen in controls, where the decline in alveolar and arterial Po_2 was approximately equal. In the oleic acid animals, the fall in alveolar Po_2 with altitude was much greater than the decline in arterial Po_2. Mean alveolar oxygen tension was 657 mmHg for all ground level conditions and averaged

478 mmHg at altitude. The difference between ground and altitude for alveolar Po_2 was 179 mmHg but only 29 mm Hg for arterial Po_2. Arterial oxygen tension, therefore, was relatively resistant to declines in alveolar Po_2. In fact, the animal with the lowest initial ground level arterial Po_2 (71 mmHg) exhibited a decrease of only 18 mm Hg to a Po_2 of 53 mm Hg at altitude. This is the corollary to the usual clinical situation seen in patients with ARDS where arterial Po_2 is relatively insensitive to increases in inspired oxygen concentrations.

Although the arterial Po_2 was relatively insensitive to changes in inspired O_2, the magnitude of the lack of responsiveness varied considerably. Since all oleic acid animals received 100% oxygen, none were severely hypoxemic at sea level, but 3 of the animals had arterial Po_2's below 100 mmHg at sea level, indicating extremely severe lung injury. The other animals had arterial Po_2's ranging from 100 to 400 mmHg, suggesting a milder degree of lung damage. These latter animals had a greater fall in arterial Po_2 with altitude. Many patients with ARDS require less than 100% oxygen, but still maintain arterial Po_2's in the range reported in our study. We cannot predict with any certainty the magnitude of change in Po_2's of patients with a wide range of lung injuries with respect to changes in inspired oxygen concentration.

Since it is difficult to predict the consequent fall in arterial oxygenation if patients had to be transported under

conditions which would result in lowered inspired Po_2, recommendations regarding oxygen levels required for maximum safety during air transport must be conservative. The decrease in oxygenation occurring in patients undergoing aeromedical evacuation would be a function of the mixed venous oxygen tension, the degree of ventilation-perfusion inequality, and the magnitude of right-to-left shunt. These factors could vary widely from one patient to another.

From these considerations it is apparent that, if a patient requires 100% oxygen at ground level and has an arterial Po_2 less than 100 mmHg, there is considerable risk that severe hypoxemia may develop during air transportation. This hypoxemia could adversely affect the likelihood of successful aeromedical evacuation. The best means of ensuring adequate oxygenation in patients who are being evacuated by air is to maintain the inspired oxygen tension at a value that produces adequate oxygenation at ground level. All that is required is to increase the inspired oxygen concentration at altitude to a level which will counteract the decrease in barometric pressure.

Fig. 12 is a guide to therapy for patients requiring supplemental oxygen during aeromedical evacuation. This figure indicates the inspired oxygen fraction which is necessary to maintain inspired Po_2 at the same value present at sea level. For example, inspired Po_2 can be maintained at 150 mmHg at a simulated altitude of 8,000 ft if inspired oxygen is increased to

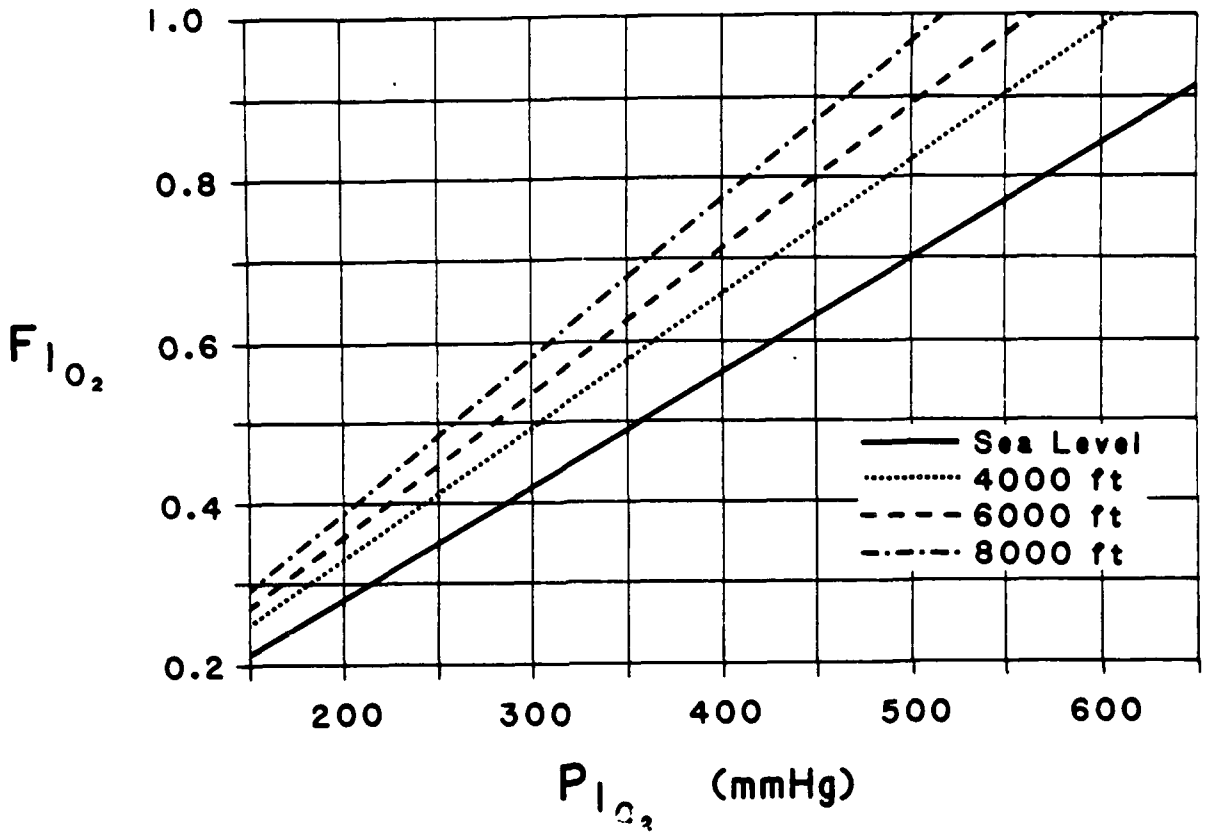

Figure 12. Relationship between inspired oxygen tension at ground level and the inspired oxygen fraction required at altitude to provide the same inspired oxygen tension that was present at ground level.

---

just under 30%. If 50% oxygen were required to maintain adequate O_2 exchange at sea level, then approximately 70% oxygen would be necessary at 8,000 ft. If the inspired oxygen fraction at sea level exceeds .725, the equivalent inspired Po_2 cannot be achieved at 8,000 ft, which suggests an upper limit in oxygen concentration for patients being evaluated for possible

aeromedical evacuation. If greater than 70% oxygen is needed at sea level to maintain satisfactory oxygenation, significant deterioration in oxygenation may occur at altitude, even if 100% O_2 is inspired. This could adversely affect patient survival. The risk-benefit ratio of transporting such a patient would have to be carefully weighed.

This approach to oxygen therapy depends upon the ability to measure arterial blood gases prior to evacuation. Under extremely adverse circumstances, it may not be possible to measure arterial blood gases. If this is the case, the most expedient approach would be to administer 100% oxygen to all severely ill patients requiring mechanical ventilation regardless of whether CMV or HFV is used to support the patient. The risk of producing oxygen toxicity while breathing 100% oxygen for durations less than 24 hours is small in normal individuals. However, little data are available to predict the effect of pure oxygen in a patient who already has an existing lung lesion. Nevertheless, it seems likely that this risk is less serious than the consequences of possible severe hypoxemia.

REFERENCES

1. Kirby, R.R.; A.J. DiGiovanni; R.W. Bancroft; and R.G. McIver. Function of the Bird respirator at high altitude. Aerospace Med 40:463-469 (1969).

2. Drazen, J.M.; R.D. Kamm; and A.S. Slutsky. High-frequency ventilation. Physiol Rev 64:505-543 (1984).

3. Chang, H.K. Mechanisms of gas transport during ventilation by high-frequency oscillation. J Appl Physiol 56:553-563 (1984).

4. Handbook of Chemistry and Physics. Ed. by R.C. Weast. Cleveland, Ohio: The Chemical Rubber Co., 1972, pp. F9-11.

5. Rossing, T.H.; A.S. Slutsky; R.H. Ingram, Jr.; R.D. Kamm; A.H. Shapiro; and J.M. Drazen. CO_2 elimination by high-frequency oscillations in dogs--effects of histamine infusion. J Appl Physiol 53:1256-1262 (1982).

6. Wagner, P.D.; P.F. Naumann; and R.B. Laravuso. Simultaneous measurement of eight foreign gases in blood by gas chromatography. J Appl Physiol 36:600-605 (1974).

7. Snedecor, G.W.; and W.G. Cochran. Statistical Methods. Seventh Edition. Iowa City: Iowa Press, 1980, pp. 267-269.

8. Prewitt, R.M.; J. McCarthy; and L.D.H. Wood. Treatment of acute low pressure pulmonary edema in dogs. J Clin Invest 67:409-418 (1981).

9. Power, G.G. Gaseous diffusion between airways and alveoli in the human lung. J Appl Physiol 27:701-709 (1969).

10. Robertson, H.T.; J. Whitehead; and M.P. Hlastala. Diffusion-related differences in elimination of inert gases from the lung. J Appl Physiol 61:1162-1172 (1986).

11. Schmid, E.R.; T.J. Knopp; and K. Rehder. Intrapulmonary gas transport and perfusion during high-frequency oscillation. J Appl Physiol 51:1507-1514 (1981).

12. Knopp, T.J.; T. Kaethner; M. Meyer; K. Rehder; and P. Scheid. Gas mixing in the airways of dog lungs during high-frequency ventilation. J Appl Physiol 55:1141-1146 (1983).

13. Kaethner, T; J. Kohl; and P. Scheid. Gas concentration profiles along airways of dog lungs during high-frequency ventilation. J Appl Physiol 56:1491-1499 (1984).

14. Berdine, G.G.; J.L. Lehr; D.S. McKinley; and J.M. Drazen. Nonuniformity of canine lung washout by high-frequency ventilation. J Appl Physiol 61:1388-1394 (1986).

15. Gavriely, N.; and J.P. Butler. Radial and longitudinal compartmental analysis of gas transport during high-frequency ventilation. J Appl Physiol 60:1134-1144 (1986).